Wave propagation, stress relaxation, and grain-to-grain shearing in saturated, unconsolidated marine sediments

Michael J. Buckingham
Marine Physical Laboratory, Scripps Institution of Oceanography, University of California, San Diego, 9500 Gilman Drive, La Jolla, California 92093-0238 and Institute of Sound and Vibration Research, The University, Southampton SO17 1BJ, United Kingdom

(Received 1 February 1999; revised 23 February 2000; accepted 9 September 2000)

A linear theory of wave propagation in saturated, unconsolidated granular materials, including marine sediments, is developed in this article. Since the grains are unbonded, it is assumed that the shear rigidity modulus of the medium is zero, implying the absence of a skeletal elastic frame. The analysis is based on two types of shearing, translational and radial, which occur at grain contacts during the passage of a wave. These shearing processes act as stress-relaxation mechanisms, which tend to return the material to equilibrium after the application of a dynamic strain. The stress arising from shearing is represented as a random stick-slip process, consisting of a random succession of deterministic stress pulses. Each pulse is produced when micro-asperities on opposite surfaces of a contact slide against each other. The quantity relevant to wave propagation is the *average* stress from all the micro-sliding events, which is shown to be a temporal convolution between the deterministic stress, $h(t)$, from a single event and the probability, $q(t)$, of an event occurring between times t and $t+dt$. This probability is proportional to the velocity gradient normal to the tangent plane of contact between grains. The pulse shape function, $h(t)$, is derived by treating the micro-sliding as a strain-hardening process, which yields an inverse-fractional-power-law dependence on time. Based on two convolutions, one for the stress relaxation from translational and the other from radial shearing, the Navier–Stokes equation for the granular medium is derived. In a standard way, it is split into two equations representing compressional and shear wave propagation. From these wave equations, algebraic expressions are derived for the wave speeds and attenuations as functions of the porosity and frequency. Both wave speeds exhibit weak, near-logarithmic dispersion, and the attenuations scale essentially as the first power of frequency. A test of the theory shows that it is consistent with wave speed and attenuation data acquired recently from a sandy sediment in the Gulf of Mexico during the SAX99 experiment. If dispersion is neglected, the predicted expressions for the wave speeds reduce to forms which are exactly the same as those in the empirical elastic model of a sediment proposed by Hamilton. On this basis, the concept of a ''skeletal elastic frame'' is interpreted as an approximate, but not equivalent, representation of the rigidity introduced by grain-to-grain interactions. © *2000 Acoustical Society of America.* [S0001-4966(00)01112-7]

PACS numbers: 43.30.Ma, 43.30.Xm [DLB]

LIST OF SYMBOLS

a	radius of circle of contact between grains
$\mathbf{A}$	vector potential
c_0	compressional wave speed in equivalent suspension
c_p	compressional wave speed in saturated granular medium
c_s	shear wave speed in saturated granular medium
d	depth beneath seawater-sediment interface
d_0	reference depth in sediment
D	root-mean-square (r.m.s.) roughness of mineral grain
E	spring constant in Maxwell element
E_g	Young's modulus of mineral grains
$h_p(t)$	radial (compressional) material impulse response function (MIRF)
$H_p(j\omega)$	Fourier transform of $h_p(t)$
$h_s(t)$	translational (shear) material impulse response function (MIRF)
$h_s(j\omega)$	Fourier transform of $h_s(t)$
j	$\sqrt{-1}$
m	translational (shear) stress-relaxation exponent
n	radial (compressional) stress-relaxation exponent
N	porosity of granular medium
$p(t)$	acoustic pressure
$q(t)$	probability density function
t	time
t_p	radial stress-relaxation time constant
t_s	translational stress-relaxation time constant
u_g	mean grain diameter
u_0	reference grain diameter
$\mathbf{v}$	particle velocity
x,y,z	Cartesian coordinates
α_p	attenuation coefficient of compressional wave in saturated granular medium
α_s	attenuation coefficient of shear wave in saturated granular medium

β_p loss tangent of compressional wave in saturated granular medium
β_s loss tangent of shear wave in saturated granular medium
γ_p compressional rigidity coefficient
γ_s shear rigidity coefficient
Γ_p normalized compressional rigidity coefficient
Γ_s normalized shear rigidity coefficient
Δ density fluctuation
η_s translational (shear) stress-relaxation coefficient
θ strain-hardening coefficient
θ_g Poisson's ratio for mineral grains
κ_0 bulk modulus of equivalent suspension
κ_g bulk modulus of mineral grains
κ_w bulk modulus of pore fluid
λ_p radial (compressional) stress-relaxation coefficient
μ_p radial (compressional) stress-relaxation modulus
μ_s translational (shear) stress-relaxation modulus
ξ_0 residual viscosity of thin pore-fluid film between asperities
$\xi(t)$ coefficient of strain-hardening dashpot in Maxwell element
ρ_g density of mineral grains
ρ_0 bulk density of saturated granular medium
ρ_w density of pore fluid
σ internal stress
χ stress in Maxwell element
ψ scalar potential
ω angular frequency

I. INTRODUCTION

In 1956 Biot published two distinguished papers[1,2] on the propagation of stress waves in a porous elastic solid containing a compressible viscous fluid in the pore spaces. An example of such a material is a water-saturated sedimentary rock. The mineral grains in a rock are strongly bonded together to form an elastic matrix, or skeletal frame. Like any other elastic solid, the consolidated skeletal frame obeys Hooke's law. In fact, Biot begins his analysis with the stress tensor for the Hookean elastic forces acting on the frame. Later in his development, two coefficients emerge, the familiar Lamé constants of elasticity theory. One of these, the shear modulus, is a measure of the rigidity of the medium, which supports the propagation of a rotational, or shear, wave. Biot also showed that the relative motion between the pore fluid and the skeletal frame leads to two compressional waves, designated dilatational waves of the first and second kind, or colloquially as the ''fast'' and ''slow'' wave. Usually the slow wave is very heavily attenuated, making it difficult to detect experimentally.

In a series of papers, culminating in a monograph,[3] Biot's theory has been adapted by Stoll in an attempt to describe wave propagation in a saturated, unconsolidated marine sediment. Unlike a rock, the mineral particles in such a sediment are unbonded. To some extent, the grains are mobile, and recent evidence indicates that, in dry sands at least, the packing arrangement evolves slowly in time due to the presence of a propagating wave.[4] Moreover, the stresses in an unconsolidated granular material under compression appear to run through the medium along random pathways, known as force chains.[5] These pathways of high stress follow routes through the medium where the grains are in tight contact. Elsewhere, the grains are looser and the stress is lower.

Such behavior indicates that, unlike a rock, the unbonded mineral grains in an unconsolidated granular material do not form a macroscopic elastic skeletal frame. The primary forces within the unconsolidated medium arise from grain-to-grain interactions. Such interactions give rise to the force chains. In the presence of a wave, grain-to-grain shearing occurs, driven by the velocity gradient across the grain contacts. In this sense, the unconsolidated granular medium is more like a viscous fluid, where the shear flow is driven by the velocity gradient normal to the flow, rather than an elastic solid in which the stress-strain relationships are governed by Hooke's law.

If the material possesses no elastic skeletal frame, the Biot theory, including Stoll's adaptations of it, does not provide an appropriate theoretical basis for describing wave propagation in an unconsolidated granular medium. An alternative approach is needed which addresses explicitly the forces associated with grain-to-grain shearing. Recently, such a treatment was developed by Buckingham and published in two articles, hereafter referred to as I[6] and II.[7]

Although the mathematical formalism describing wave propagation in an unconsolidated sediment is established in I and II, the treatment is inductive rather than deductive. For instance, the relationship presented in I and II between internal stress and rate of strain is not deduced from a specific physical mechanism, and the general form of the Navier–Stokes equation used in the analysis is not derived in the original papers but is merely stated, largely by analogy with wave propagation in a viscous fluid.

The purpose of the present article is to rectify these deficiencies. Central to the argument is a stochastic treatment of intergranular shearing, based on a random ''stick-slip'' process. Each ''slip'' is a microscopic, stress-relaxation event between micro-asperities, which are separated by a very thin film of interstitial fluid (seawater). Recent developments in tribology[8] have established that thin aqueous films, less than about ten molecular diameters thick, exhibit an effective viscosity which is considerably higher than the viscosity of the bulk fluid and which increases rapidly as the force compressing the contact grows. It is proposed that, in a saturated granular medium, the viscosity of the lubricating fluid film between micro-asperities increases as the slip progresses, a phenomenon known as strain hardening.[9] In a granular medium, strain hardening makes a microscopic shearing event more difficult to sustain as the sliding continues.

The wave properties that derive from the random stick-slip, strain-hardening model are similar to those observed experimentally in saturated marine sediments. Since relative

motion between the pore fluid and the mineral grains is not included in the model, only one dilatational wave emerges from the theory (no slow wave is predicted), and interestingly, the new grain-shearing mechanism introduces rigidity into the medium, which weakly supports a rotational wave. Both the dilatational and the shear wave exhibit weak, near-logarithmic dispersion and an attenuation that scales, over many decades, essentially as the first power of frequency.

Before developing the model and deriving the properties of the dilatational and the shear wave, some recent experimental observations on unconsolidated granular media are reviewed. As noted by Jaeger *et al.*,[10] a (dry) granular material behaves differently from a solid, a liquid, and a gas, even though it may possess some of the properties of each. They even suggest that it represents an additional state of matter in its own right. Similar comments could be made about a saturated unconsolidated granular material, not only in connection with its mechanical behavior but also its wave properties.

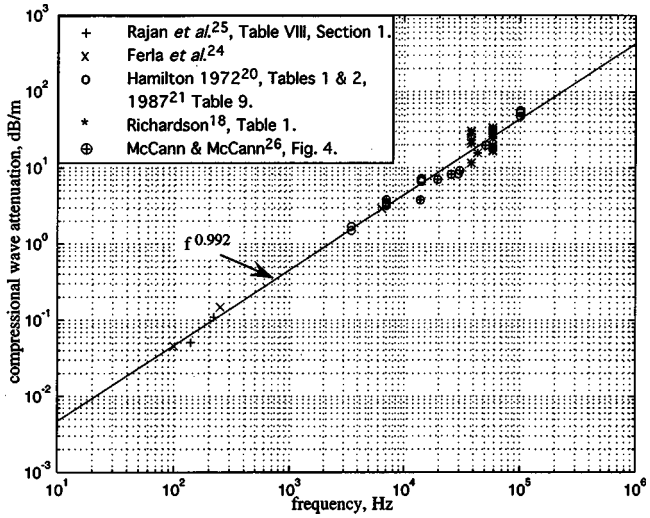

FIG. 1. Compilation of *in situ* data showing compressional wave attenuation as a function of frequency in sands. The solid line is a least-squares fit of a frequency power law to the data.

II. FORCE CHAINS

In a recent series of laboratory experiments on dry sand, Nagel and colleagues[4,5,11–14] found that granular media exhibit unique properties, most if not all of which are a result of grain-to-grain interactions. In particular, they observed that the stress in a sand pile tends to concentrate along random pathways passing through the points of contact between grains. By using a system of crossed polarizers, Liu *et al.*[5] were able to visualize the elongated regions of relatively high stress (see their Fig. 1), which they refer to as force chains.

Acoustic waves within the granular medium tend to propagate along the force chains. Since more than one force chain may connect an acoustic source and receiver buried in the medium, interference may occur between waves propagating along each of the force-chain pathways, giving rise to a received signal that fluctuates strongly with changing frequency (as illustrated in Fig. 3 of Liu and Nagel[4]). The experimental findings suggest that the contacts between mineral grains are very fragile. A minuscule mechanical disturbance to the arrangement of the grains causes a substantial change in the level of the received signal, behavior that Nagel and co-authors attribute to the shifting of the packing structure, and hence the force chain pathways, in response to a very small applied strain.

Even the presence of a propagating, small-amplitude wave introduces sufficient strain to alter the medium on a microscopic level. As a result, the level of the received signal from a single-frequency source slowly evolves in time, continually making excursions about its average value as the wave itself modifies the random arrangement of the grains in the host material. This evolutionary behavior is illustrated in Fig. 1(a) of Liu and Nagel,[4] which shows a time series, lasting approximately 8 h, of the received signal level from a 4-kHz, constant-amplitude source. Fluctuations in the level of the signal arrival can be seen to occur over a wide range of time scales.

The continuous evolution of the amplitude fluctuations suggests that, during the passage of the wave, intergranular shearing occurs continuously. Each microscopic grain-to-grain shearing event leads to a new realization of the medium, which differs almost imperceptibly from the previous realization. Since the changes are cumulative, the packing structure of the grains after a long transmission may be significantly different from the original arrangement. A summary of the experiments and conclusions from Nagel's group can be found in a recent article on waves in granular media by Nagel and Jaeger.[15]

Variability in the wave properties of granular materials is observed, not only in the laboratory, but also in wave data collected from the seabed. Using their ISSAMS frame,[16–18] Richardson and colleagues have performed numerous *in situ* measurements of compressional and shear waves in unconsolidated marine sediments. In one of their recent experiments in medium sand in the Gulf of Mexico, they observed strong fluctuations[19] in the received signal from a frequency-modulated (chirp) source. These fluctuations are much like those seen in Liu and Nagel's[4] Fig. 3. As in the laboratory experiments, interference between arrivals that propagated along two or more force-chain pathways would appear to be a plausible explanation for the origin of the fluctuations in the *in situ* measurements.

III. WAVE PROPERTIES OF UNCONSOLIDATED SEDIMENTS

Spot-frequency measurements of wave attenuation in sediments exhibit considerable scatter, possibly due partly to the slow evolution of arrival amplitudes. Consequently, most authors adopt a statistical approach when reporting attenuation data. Thus Hamilton,[20,21] Wood and Weston,[22] and Bjørnø,[23] have reported measurements of the average attenuation of the compressional wave as a function of frequency in unconsolidated marine sediments. Over limited frequency ranges, they all found that the attenuation scales as f^s, where the index s is close to unity.

This linear scaling with frequency is exemplified in Fig. 1, which shows a compilation of compressional wave attenu-

ation data for saturated sands. The data points in the figure are from tables in Hamilton,[20,21] Richardson,[18] Ferla *et al.*,[24] and Rajan *et al.*,[25] and from Fig. 4 in McCann and McCann.[26] All the data points in Fig. 1 were collected *in situ* and are representative of the sediment just beneath the sea floor. No data from laboratory measurements, or from deep in the sediment, or from materials other than sand, appear in Fig. 1. The solid curve in Fig. 1 is a power-law, least-squares fit to the data, which varies as $f^{0.992}$. The near-linear scaling of the attenuation with frequency, f, is clearer in Fig. 1 than in some of Hamilton's plots, which superimpose data from all types of sediment (sands, silt/sands, silts, and clays), data taken *in situ* and under laboratory conditions, and data taken at great and shallow depths.

In a recent survey article, Bowles,[27] in his Fig. 1, plotted a compilation of data showing compressional wave attenuation as a function of frequency in fine-grained sediments, mostly muds, clays, and turbidites. Over a frequency range extending from 10 Hz to 500 kHz he found that the attenuation exhibits a near-linear scaling with frequency: his best power-law fit to the data varies as $f^{1.12}$.

No published, *in situ* measurements are known on the frequency dependence of the shear wave attenuation in sands. Laboratory measurements of shear wave attenuation in a water-saturated medium sand, from Table II in Brunson and Johnson,[28] are shown in Fig. 2(a). The solid line, varying as $f^{1.11}$ and passing through the data points, is a least-squares fit of a frequency power law to the data. Although Brunson and Johnson[28] themselves suggest otherwise, the shear attenuation data appear to exhibit a near-linear scaling with frequency over the bandwidth (0.45 to 7 kHz) of the experiment.

Brunson[29] found similar behavior for the attenuation of the shear wave in water-saturated, sorted glass beads. Figure 2(b) shows the data from his Table 2, along with a least-squares fit of a frequency power law varying as $f^{1.06}$. Curiously, Brunson[29] interpreted the measurements in Fig. 2(b) as showing ''evidence of viscous attenuation due to fluid-to-grain relative motion.'' This unfortunate statement, which has been accepted at face value in at least one review article,[30] does not appear to be consistent with the data in Fig. 2(b). These shear attenuation data can be seen to exhibit a near-linear dependence on frequency over a band from 1 to 20 kHz.

A medium with an attenuation that essentially scales with frequency should, according to the Kramers–Kronig relationships, exhibit near-logarithmic dispersion.[31–36] The level of the dispersion is proportional to the loss tangent (or inversely proportional to the Q) of the material and, for the compressional wave in a typical sand, is in the region of 1.5% per decade of frequency. This is too low to be detected in many experiments, even under laboratory conditions.

Nevertheless, several investigators have attempted to detect the frequency dependence of the compressional wave speed in sand.[20,37,38] All concluded that dispersion, if present at all, is very weak. In a more recent laboratory experiment, Wingham[39] observed logarithmic dispersion at a level of approximately 1% per decade in a medium sand over a frequency range between 100 and 350 kHz. Although this bandwidth is limited, Wingham's observation is not inconsistent with the Kramers–Kronig requirement for a material with an attenuation that scales linearly with the frequency.

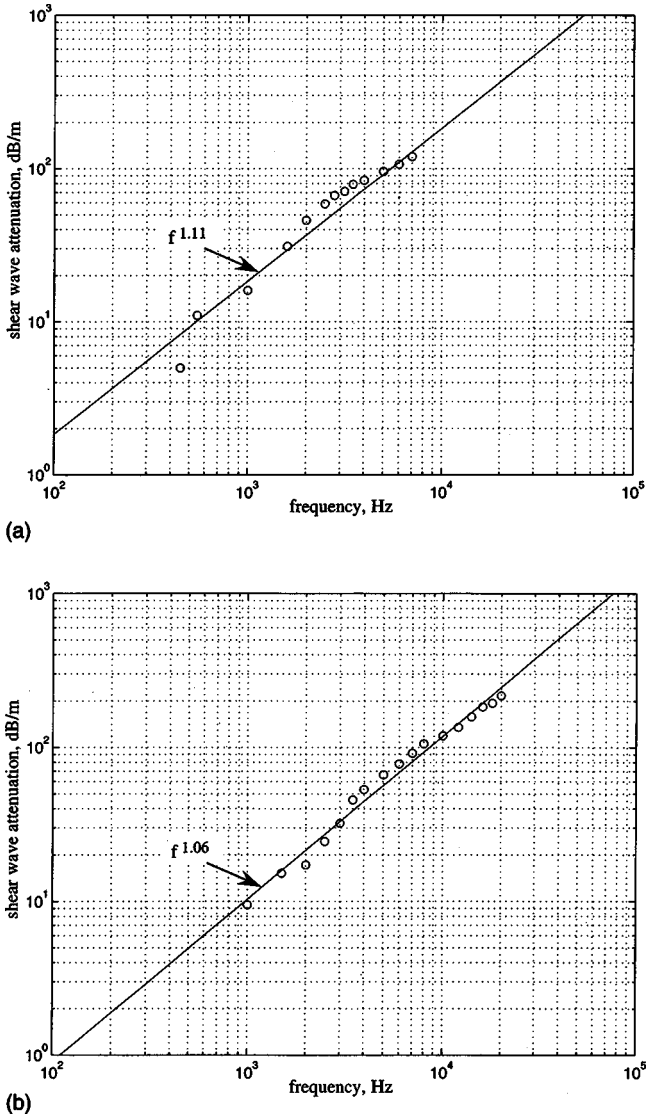

FIG. 2. Laboratory data showing the attenuation of the shear wave as a function of frequency and a least-squares fit of a frequency power law. (a) Saturated medium sand, data from Brunson and Johnson (Ref. 28). (b) Saturated glass beads, data from Brunson (Ref. 29).

In a critical discussion of the published experimental evidence on frequency dispersion in sands and sediments, Hamilton[20] concluded that ''velocity dispersion is negligible or absent in water-saturated sediments.'' He was also of the opinion that wave attenuation in marine sediments is dominated by grain-to-grain interactions, which is consistent with the observations of force-chains in dry sands by Nagel and colleagues. Viscous losses associated with the relative movement of the pore fluid through the mineral structure, the primary dissipation mechanism in the Biot theory, were considered by Hamilton[20] to be negligible. He based this conclusion on the fact that the velocity dispersion is negligible, which would not be the case if viscous dissipation were significant.

A secondary piece of evidence indicating that viscous flow has little effect on wave propagation was reported by

Wyllie *et al.*[40] They found that the speed of compressional waves through water-saturated glass beads remained unchanged as the permeability was varied by a factor of 4.6 $\times 10^4$. This insensitivity to the permeability implies that relative motion between the viscous pore fluid and the unbonded mineral grains is insignificant.

If the flow of pore-fluid between grains is negligible, the slow wave predicted by the theory of Biot[1,2] and its modifications by Stoll[3] should be extremely weak, if not absent altogether. A steadily accumulating body of experimental evidence indicates that this is indeed the case. Despite several attempts to detect it under controlled laboratory conditions,[41–46] the slow wave in unconsolidated, saturated granular media has never been observed. (The slow wave has been detected in a *consolidated* porous medium consisting of lightly fused glass spheres).[45,46]

Hamilton's[20] contention that grain-to-grain interactions largely determine the properties of waves in unconsolidated granular media is supported by the fact that the compressional and shear wave speeds show a pronounced dependence on grain size. Experimental data, compiled from a number of published sources and showing the functional dependence of compressional and shear wave speeds on grain size, are plotted, respectively, in Fig. 8 in I and Fig. 5 in II. Similar grain-size data, acquired using the ISSAMS frame, have been presented by Richardson,[18] who fitted empirical curves to the experimental points using a regression analysis.

Not all the published evidence is unequivocal in supporting grain-to-grain interactions as being responsible for the wave properties of saturated granular materials. For instance, Simpson and Houston[44] recently reported laboratory measurements of the dispersion and attenuation of the compressional wave in a fine-to-medium sand over the frequency range 4 to 100 kHz. Their acoustic source was in the water column above the sediment and a single hydrophone buried in the sand was moved systematically from run to run to form a synthetic-aperture receiver array. The attenuation was found to vary approximately as $f^{0.61}$, a slope that is somewhat slower than would be expected from grain-to-grain interactions. Dispersion, on the other hand, was not evident in the sound-speed data, which is consistent with a grain-to-grain argument.

It is quite possible that more than one mechanism is responsible for the wave properties of saturated, unconsolidated granular media. Nevertheless, from the weight of experimental evidence that has accrued over the years, it is difficult to avoid the conclusion that grain-to-grain interactions play an important role in characterizing wave behavior in these materials. The remainder of the paper is devoted to developing a model of grain-to-grain shearing, which, as will be shown, gives rise to many of the observed properties of waves in unconsolidated sediments.

IV. THE MODEL

It is assumed that the unconsolidated, saturated granular material consists of mineral grains of essentially uniform size, that there are no large inclusions such as shell fragments that would act as scattering centers, that there is no gas in the pores, and that the wavelength is considerably longer than the size scale of the grains and pore spaces. Taking the grain boundaries as orientated randomly throughout, the medium is treated as statistically homogeneous and isotropic. Boundary reflections are assumed to be negligible. No skeletal mineral frame is included in the analysis, that is to say, the elastic rigidity modulus of the medium is taken to be zero. (The elasticity of the mineral grains themselves is not neglected.) In effect, the granular medium is treated as a fluid in which the stress-strain relationships are governed by shearing at the embedded grain contacts. It is implicit in these assumptions that only intrinsic attenuation is addressed in the model. Phenomena such as high-frequency scattering from individual grains are excluded from the analysis.

By treating the medium as a homogeneous continuum, it is implicit that relative motion between the viscous pore fluid and the mineral grains is neglected in the model. This is the ''closed system'' of Gassmann[47] in which the pore fluid does not circulate between grains under the influence of the very low stress from a propagating wave. The absence of viscous flow through the pore spaces has several consequences, the most obvious being that the model does not lead to a slow wave of the type that emerges from the Biot theory. Another is that the predicted wave properties are independent of the permeability, the tortuosity, and the structure factor, which in the Biot–Stoll treatment characterize the fluid flow between the grains. In the grain-shearing theory, the material parameter which governs the wave properties is the porosity, which is commonly reported along with the wave properties of unconsolidated granular materials.

Central to the theoretical development is the shearing that occurs at grain contacts during the passage of a wave. On a microscopic level, the contacts themselves are taken to be at discrete high points, that is, at micro-asperities on the nominally smooth surface of the grains. Each such microcontact is assumed to be lubricated by a very thin layer of pore fluid. When sliding occurs at one of these points of contact, the drag opposing the motion is not due to dry friction, but to the effective viscosity of the thin lubricating fluid film, which may be considerably higher than the viscosity of the bulk fluid.

The model is statistical in the sense that many microasperities contribute randomly in time to the shearing. An ensemble average over all the shearing events provides the basis for determining the relationship between stress and strain in the medium. This relationship turns out to be a convolution integral, one term of which is a material impulse response function, or MIRF. In fact, two MIRFs appear in the analysis, corresponding to the two types of shearing that can occur between grains. In effect, a MIRF is the stress relaxation that occurs in the material in response to a step-function strain or, equivalently, an impulse of strain rate.

The stress-strain convolutions appear in the Navier–Stokes equation of motion, which splits into two equations, one for compressional and the other for transverse disturbances. Both are genuine wave equations, implying that grain shearing introduces rigidity into the medium, and the rigidity supports a shear wave. Dissipation is also associated with grain shearing, which gives rise to an attenuation in

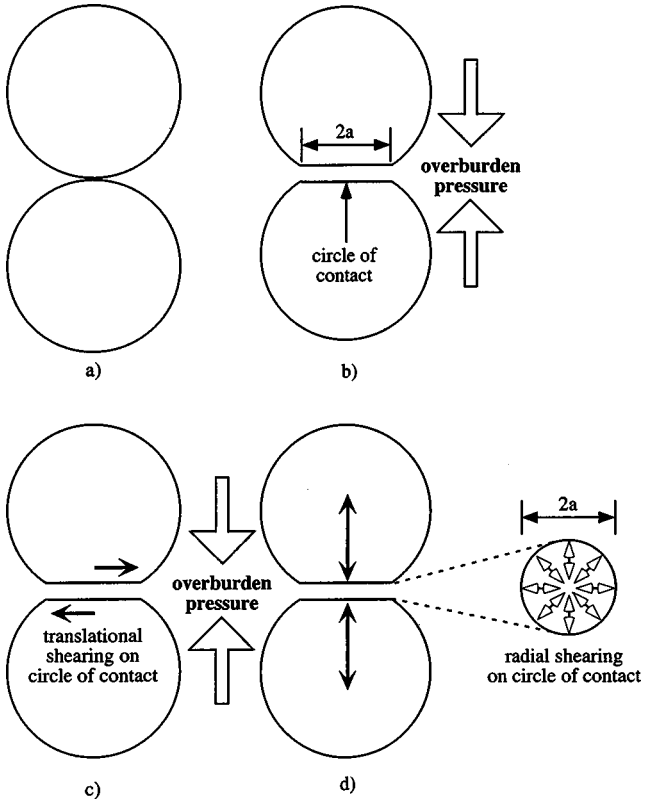

FIG. 3. Cross section through the centers of two contiguous, spherical, mineral grains. (a) Touching lightly, with no elastic deformation at the point of contact. (b) Pressed together by static overburden pressure, elastic deformation occurs, creating a small circle of contact. (c) Translational shearing due to dynamic tangential strain (horizontal black arrows) and (d) compressive shearing along radials of the circle of contact (small open arrows) due to dynamic normal strain (vertical black arrows).

both waves that scales essentially as the first power of frequency.

V. GRAIN-BOUNDARY SHEARING

Since shearing between grains is central to the model, it is important to consider how such shearing may occur. Figure 3(a) is a schematic of two identical elastic spheres in light contact. The spheres are an idealization of contiguous mineral (often quartz) grains in a sediment. When a static force, F, is applied normal to the tangent plane of contact, the grains are pressed together, local elastic deformation occurs, and a small circle of contact is formed [Fig. 3(b)]. In a sediment, the force F may be identified with the overburden pressure.

During the passage of a wave, a small, dynamic, elastic deformation takes place in the vicinity of the contact in addition to the static deformation illustrated in Fig. 3(b). The result of the dynamic deformation is relative motion (shearing) between the two grains. The shearing relieves the stress produced by the wave and tends to restore equilibrium between the grains. Two types of shearing may occur: translational shearing and radial shearing, illustrated in Figs. 3(c) and (d), respectively.

Under translation, the grain centers are displaced relative to each other in a direction parallel to the tangent plane of contact. In response to this shear strain, tangential shear stress relaxation occurs as micro-asperities slide against one another on the surfaces of the circles of contact. Radial shearing occurs under compressive or tensile strain, that is, when the grain centers are displaced in a direction normal to the tangent plane of contact. Such normal strains produce compressional (tensile) stress relaxation as micro-asperities on the radials of the circle of contact slide against one another. It is to be emphasized that, for typical stress waves in a sediment, the translational and radial displacements are extremely small, corresponding to strains of 10^{-6} or less.

In passing, it should be mentioned that if the two spheres in Fig. 3 were smooth and of the same size, then the shearing along the radials of the circle of contact due to compression (tension) would be zero: the two spheres would deform identically, and no radial sliding would occur. In practice, sliding will be present even when the spheres are of the same size because sand grains are not perfectly smooth but are covered with randomly distributed, microscopic asperities. Note also that radial shearing will occur under not only positive (compressional) but also negative (tensile) dynamic strains. These positive and negative strains produce very small excursions about the equilibrium state maintained by the overburden pressure. Radial shearing occurs under dynamic tension because of the slight relaxation of the deformations on either side of the contact, and under dynamic compression because of the slight enhancement of those same deformations.

The presence of micro-asperities means that the contact between the two spheres is not perfect. Based on recent advances in tribology,[48] it is expected that many discrete points of contact will exist, distributed randomly over the rough surfaces of the circle of contact. A similar situation has been described by Bengisu and Akay[49] in their analysis of friction at microscopically rough surfaces. When grain-to-grain shearing occurs in response to a dynamic strain, stress relaxation occurs at the microscopic points of contact. The shearing events are triggered randomly in time with a probability that depends on the normal gradient of the strain across the micro-contact. The resultant random sequence of discrete, stress-relaxation pulses constitutes the mechanism by which equilibrium between two grains is restored.

According to this picture, in the presence of a wave, as the stress relaxation proceeds, the micro-geometry of the surfaces of contact changes irreversibly. After a microscopic sliding event, the disposition of the two asperities involved is slightly different from beforehand. These minute changes on the circle of contact are cumulative, and are thus expected to produce a slowly evolving grain-packing structure as wave propagation through the medium continues. Such behavior appears to be consistent with the stochastic properties of waves in dry granular media observed by Nagel and colleagues. It seems evident that the slow evolution of the packing structure from micro-slip events could be responsible for a changing pattern of force chains within the granular material. The expected result would be fluctuations in the amplitude of signal arrivals, much like those observed over a period of several hours by Liu and Nagel[4] and illustrated in their Fig. 1(a).

VI. RANDOM STICK-SLIP STRESS RELAXATION

To model the stress relaxation that occurs as two grains slide against each other, the process is represented as a random succession of pulses. Each pulse is the deterministic stress arising from the slippage of one microscopic asperity past another on the circle of contact. The sliding is triggered by the normal velocity gradient across the contact due to the wave disturbance itself. Once triggered, the pulse amplitudes are taken to be independent of the velocity gradient. Since the micro-pulses of stress are the fundamental constituents of both translational [Fig. 3(c)] and radial [Fig. 3(d)] shearing, an identical argument applies to the two cases.

The stress relaxation associated with a particular micro-shearing event occurring at time $t=0$ is represented by the pulse shape function, $h(t)$, where, to satisfy causality, $h(t)=0$ for $t<0$. Letting t_k be the time at which the kth event of amplitude a_k occurs, the total stress from the random succession of events may be written as

$$\sigma(t)=\sum_{k=1}^{\infty} a_k h(t-t_k), \tag{1}$$

where the onset times, t_k, and the time-independent amplitudes, a_k, are random variables, all of which are taken to be independent of one another. The summation on the right of Eq. (1) is known as a random pulse train.[50]

Within an elementary volume of the granular medium, which is large compared with the grain size but small relative to a wavelength, many grain contacts are expected to exist, and thus the quantity of interest in connection with the macroscopic wave properties is the average stress over a large number of contacts. The mean stress is derived below as an ensemble average of the random pulse train in Eq. (1), following a generalized version of the argument that holds for the more familiar Poisson process.[51]

Consider shearing at a single grain boundary. During an observation interval $[0,T]$, the probability of a particular micro-sliding event occurring between times t and $t+dt$ is

$$\nu dt=\overline{K}q(t)dt, \tag{2}$$

where $\overline{K}$ is the average number of events in time interval T, and $q(t)$ is a function of time that satisfies the condition

$$\int_0^T q(t)dt=1, \tag{3}$$

because the event must occur sometime during the interval $[0,T]$. Note that the probability in Eq. (2) is independent of what occurred before time t and what will happen after time $t+dt$. A Poisson process would have $q(t)=1/T$, a constant, and ν would be the mean rate of events, that is, $\overline{K}/T$. The random stick-slip that occurs at a grain boundary is not, however, Poisson distributed, but is triggered by the velocity gradient across the boundary at any instant, t. Thus the probability density function, $q(t)$, is governed by the instantaneous magnitude of the wave field in the medium: the greater the velocity gradient, the more likely that a slip will be triggered.

To perform the required averaging of Eq. (1), consider the random pulse trains associated with a very large number, M, of observation intervals, each of duration T. If $p(K)$ is the probability of an interval in the ensemble containing *exactly* K events, then the number of such intervals is $Mp(K)$. Thus at a fixed time t into each interval, as $M\to\infty$, the average value of the stress, $\sigma_K(t)$, in the intervals containing *exactly* K events is

$$\begin{aligned}\overline{\sigma_K(t)}&=\overline{a_K}\int_0^T q(t_1)dt_1\cdots\int_0^T q(t_K)dt_K\sum_{k=1}^{K} h(t-t_k)\\&=\overline{a_K}\sum_{k=1}^{K}\int_0^T q(t_k)h(t-t_k)dt_k\\&=\overline{a_K}K\int_0^T q(t_k)h(t-t_k)dt_k,\end{aligned} \tag{4}$$

where the overbar denotes an ensemble average, and $\overline{a_K}$ is the mean value of the pulse amplitudes a_k in the intervals containing exactly K events. Note that the stress-relaxation amplitudes, a_k, will all have the same sign and hence $\overline{a_K}\neq 0$. The final expression in Eq. (4) holds because the integral is independent of the index k and hence may be taken outside the summation.

Now, the average value of the stress relaxation in *all* the intervals $[0,T]$ is

$$\overline{\sigma(t)}=\sum_{K=1}^{\infty} p(K)\overline{\sigma_K(t)}=\overline{a}\int_0^T q(t_k)h(t-t_k)dt_k\sum_{K=1}^{\infty} Kp(K). \tag{5}$$

The summation in the last expression is simply the mean number of events in the interval $[0,T]$,

$$\overline{K}=\sum_{K=1}^{\infty} Kp(K), \tag{6}$$

an expression which holds for any probability distribution $p(K)$, and hence

$$\overline{\sigma(t)}=\overline{a}\,\overline{K}\int_0^T q(t_k)h(t-t_k)dt_k, \tag{7}$$

where $\overline{a}\neq 0$ is the mean value of the pulse amplitudes in all the intervals $[0,T]$. Equation (7) is an ensemble average for the mean stress relaxation that occurs when one grain slides against another. Notice that the onset time, t_k, of the kth event in the random pulse train is the integration variable in Eq. (7), that is to say, the distribution of the onset times has no effect on the value of the average.

In view of the fact that the probability $q(t_k)=0$ for $t_k<0$ and $h(t)=0$ for $t<0$, the limits on the integral in Eq. (7) may be extended from $-\infty$ to $+\infty$ without changing its value,

$$\overline{\sigma(t)}=\overline{a}\,\overline{K}\int_{-\infty}^{\infty} q(t_k)h(t-t_k)dt_k. \tag{8}$$

The integral on the right of Eq. (8) will be recognized as a convolution integral, allowing the average stress to be expressed in the form

$$\overline{\sigma(t)}=\overline{a}\,\overline{K}q(t)\otimes h(t), \tag{9}$$

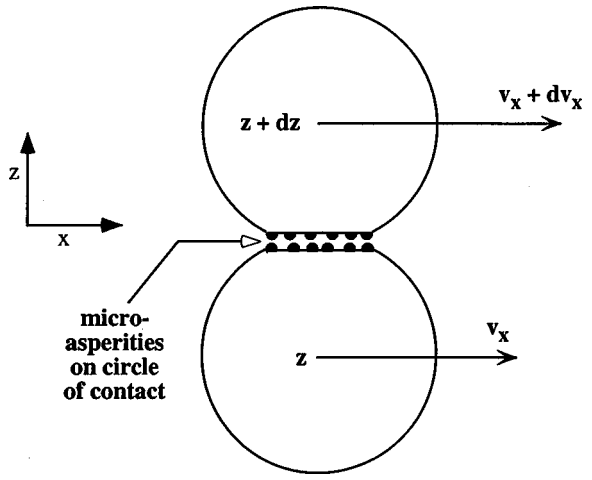

FIG. 4. Shearing of contiguous grains due to the velocity gradient normal to the plane of contact. The micro-asperities (small solid hemispheres) on the circle of contact are not to scale.

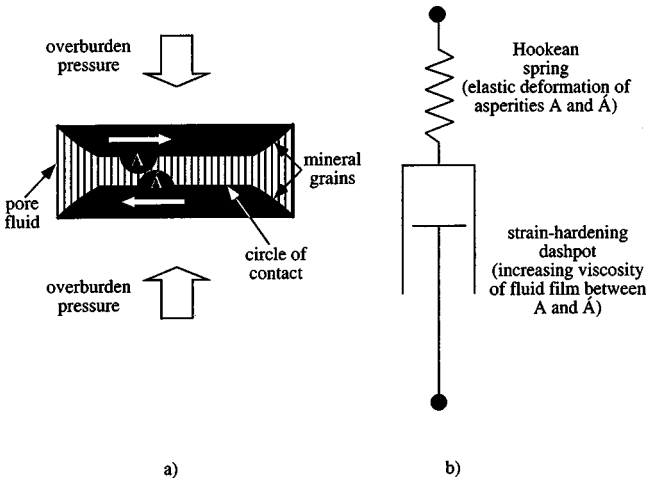

FIG. 5. (a) Asperities A and $\acute{A}$ shearing against each other (not to scale) on the circle of contact. A thin film of pore fluid is shown between A and $\acute{A}$. (b) Equivalent Maxwell element consisting of a Hookean spring and nonlinear, strain-hardening dashpot in series.

where the symbol $\otimes$ denotes a temporal convolution. Equation (9) is a generally valid result for any random pulse train for which the probability density function is $q(t)$ and the pulse shape function is $h(t)$. To proceed, it is necessary to determine the functional forms for $q(t)$ and $h(t)$ that are appropriate to grain-to-grain shearing in an unconsolidated granular medium.

VII. THE PROBABILITY DENSITY FUNCTION, $q(t)$

It is clear that the difference in velocity of the two grains on either side of the circle of contact must trigger the stick-slip process. When boundary shearing occurs, the grain centers move relative to each other in a direction which may be resolved into components parallel to (translational shearing) and normal to (radial shearing) the tangent plane of contact. Similar arguments apply to the two cases, but to be specific we shall discuss the probability function $q(t)$ in the context of translational shearing.

To establish the form of $q(t)$, consider for the moment just two-dimensional motion in the $x-z$ plane, with the plane of the contact parallel to the x-direction, as sketched in Fig. 4. The density function, $q(t)$, is the probability that a single micro-shearing event will contribute to the stress relaxation between times t and $t+dt$. Since each event is triggered by the magnitude of the velocity difference across the plane of contact, the probability that a given event occurs between times t and $t+dt$ is

$$q(t)=\frac{b}{T}\left|\frac{dv_x(t)}{dz}\right|, \tag{10}$$

where b is a (positive) constant of proportionality, and the derivative on the right is the velocity gradient normal to the grain boundary at time t. To account for planes of contact that are not parallel to the x-direction, b may be replaced by its average value, $\bar{b}$, taken over the random orientation of the slip planes,

$$q(t)=\frac{\bar{b}}{T}\left|\frac{dv_x(t)}{dz}\right|. \tag{11}$$

By writing the velocity as $v_x=dx/dt$, it becomes evident that the derivative in Eqs. (10) and (11) is identical with the rate of strain across the contact. Thus the probability of an event occurring between t and $t+dt$ is proportional to the rate of strain rather than the strain itself, which is physically reasonable since a static strain represents a steady-state condition in which no shearing could occur.

When the expression in Eq. (11) is substituted into Eq. (9), the average stress becomes

$$\overline{\sigma_{xz}(t)}=\nu\bar{a}\bar{b}\left|\frac{dv_x(t)}{dz}\right|\otimes h(t), \tag{12}$$

where $\nu=\bar{K}/T$ is the mean rate of sliding events and the subscripts xz on the left denote in the usual way the shear stress in the $x-z$ plane. An analogous expression holds for radial shearing, in which case the subscript x is replaced by z.

VIII. STRAIN HARDENING AND THE PULSE SHAPE FUNCTION, $h(t)$

The pulse shape function, $h(t)$, is a deterministic, material impulse response function (MIRF). It represents the time dependence of the stress relaxation that occurs as one micro-asperity slides against another in response to an impulse of strain rate.

Two forces are at work when individual asperities on opposite faces of the circle of contact slide against each other: a conservative elastic force of deformation, and a drag force resisting the motion [Fig. 5(a)]. The elastic force may be represented by a simple Hookean spring. Opposing the motion, the drag force is due to friction from the viscosity of the thin film of pore fluid trapped between the asperities. Viscous drag scales with the speed of sliding, and hence may be represented by a dashpot. Since they support the same stress, the spring and the dashpot should be connected in series [Fig. 5(c)] to represent the micro-shearing, a combination which is sometimes known as a Maxwell element.[9] Usually, a Maxwell element is employed to represent the elastic or plastic behavior of a macroscopic sample of the material

of interest but, in the present instance, it serves as an equivalent mechanical model of the micro-sliding between individual asperities on the circle of contact.

In its simplest form, the coefficients of the spring and dashpot in the Maxwell element are constants, in which case the MIRF, $h(t)$, would decay exponentially in time. Such behavior, however, is not characteristic of the stress relaxation that occurs in granular media. The physical processes underlying the grain-to-grain interactions in granular materials are still not well understood, although the subject has received considerable attention,[52–56] as summarized in a review article by Deresiewicz.[57] Much of this prior work addresses the contact mechanics of elastic spheres arranged in regular arrays. A different approach is taken here, where it is postulated that ''strain hardening,'' originating in the thin fluid film separating two sliding asperities, may be the mechanism that governs the properties of waves in unconsolidated granular media.

Strain hardening is an increase in the resistance to motion as intergranular shearing proceeds. Thus after it is triggered, the shearing becomes progressively more difficult to sustain, behavior which is represented by a time-dependent coefficient for the dashpot in the Maxwell element in Fig. 5(b). It is well-known that a Maxwell element in which the dashpot hardens with time can exhibit behavior that is representative of stress relaxation in plastic materials, as discussed in a number of contexts by Gittus.[9] However, since a granular material is not plastic, at least, not in the usual sense, the details of the strain hardening mechanism will differ in the two cases.

The thinness of the pore fluid sandwiched between the asperities depicted in Fig. 5(a) could be responsible for strain hardening in the granular medium. It is known that the properties of aqueous solutions confined in a very thin layer (several molecular diameters thick) between solid surfaces are significantly different from those of the bulk material.[8] In particular, the effective viscosity of a thin fluid film can be much higher than the viscosity of the bulk fluid, and the effective viscosity increases as the film is squeezed harder.[48,58] This may be what happens as the asperities A,$\acute{A}$ in Fig. 5(a) slide against each other.

Before sliding begins, the two asperities are effectively pinned (the ''stick'' part of ''stick-slip''). On being triggered into slipping, the contact between the two asperities will always become tighter, because of the overburden pressure, and the effective viscosity of the lubricating fluid film will increase, giving rise to the condition of strain hardening. In terms of the Maxwell element in Fig. 5(b), the strain hardening is represented by allowing the coefficient of the dashpot, $\xi(t)$, to be an increasing function of time. Since the stress in such a dashpot is neither in phase nor in quadrature with the strain, the element is not purely dissipative, as it would be if the coefficient were constant. In fact, the strain-hardening dashpot is nonlinear, with cross-coupling between different Fourier components in the stress-strain relationship, and hence the Maxwell element in Fig. 5(b) does not obey the principle of superposition.

The coefficient of the spring in the Maxwell element is taken to be a constant, E, representing the compressibility of the asperities A,$\acute{A}$ and the fluid film between them. It should be noted that, although the compressibility of the bulk pore fluid is considerably greater than that of the mineral grains, the situation may be reversed for the molecularly thin film of pore fluid between asperities. As discussed by Granick,[8] such thin fluid films are highly incompressible. Thus as indicated in Fig. 5(b), the predominant factor governing the spring constant E may actually be the elasticity of the mineral asperities rather than the compressibility of the pore fluid separating them.

Be that as it may, the solution for the stress in the Maxwell element in response to a step-function strain, ε, applied at $t=0$ will provide an expression for the MiRF $h(t)$. The applied strain, ε, is governed by material properties alone, that is to say, it is taken to be independent of the wave amplitude.

Since they are in series, the stresses in the spring and the dashpot are the same. Taking the stress at time t to be $\chi = \chi(t)$, then in the spring

$$\chi = E\varepsilon_s, \tag{13}$$

which is simply Hooke's law, and in the strain-hardening dashpot

$$\chi = \xi(t)\frac{d\varepsilon_d}{dt}. \tag{14}$$

In these expressions, ε_s and ε_d, respectively, are the time-dependent strains in the spring and the dashpot. After $t=0$ the total strain, ε, in the Maxwell element is just the sum of the strains in the two components,

$$u(t)\varepsilon = \varepsilon_s + \varepsilon_d, \tag{15}$$

where $u(t)$ is the unit step function. On combining Eqs. (13) to (15), the following nonlinear differential equation for the stress, χ, is obtained:

$$\frac{1}{E}\frac{d\chi}{dt} + \frac{1}{\xi(t)}\chi = \varepsilon\,\delta(t), \tag{16}$$

where $\delta(t)$ is the Dirac delta function.

To solve Eq. (16) for the stress, the time-dependence of $\xi(t)$, the coefficient of the dashpot, must be specified. The Taylor expansion of this coefficient about time $t=0$ when sliding begins is

$$\xi(t) = \xi_0 + \left.\frac{d\xi}{dt}\right|_{t=0} t + \left.\frac{d^2\xi}{dt^2}\right|_{t=0}\frac{t^2}{2!} + \cdots \approx \xi_0 + \theta t, \tag{17}$$

where the zero-order term, ξ_0, represents the viscosity of the fluid film before the onset of sliding, and $\theta \geqslant 0$ is the strain-hardening coefficient or, equivalently, the rate coefficient of the drag. The linear approximation for $\xi(t)$ in Eq. (17) would seem to be justified, given the very short time scales and extremely small strains associated with linear wave propagation in granular media. Later, it will be shown that the theoretical results derived on the basis of the approximation in Eq. (17) agree with the available experimental data.

By employing the linear form in Eq. (17), the solution of Eq. (16) is obtained, after rearranging terms, by straightforward integration,

$$\chi = \chi_0 \left(1 + \frac{\theta}{\xi_0} t \right)^{-E/\theta} \mathrm{sgn}[\varepsilon \delta(t)], \tag{18}$$

where

$$\chi_0 = |\varepsilon| E \tag{19}$$

is the initial value of the stress, $\delta(t)$ is the Dirac delta function, and the signum function represents the arithmetic sign of the driving rate of strain. Equation (18) states that at $t = 0+$ all the strain appears across the spring, as expected because the dashpot cannot respond instantaneously to the input. Note that the limiting behavior of the solution in Eq. (18) is correct: as $\theta \to 0$ (i.e., as the effect of strain-hardening is eliminated), χ reduces identically to an exponential decay in time. When, in addition, the elasticity is removed by allowing $E \to \infty$, χ becomes the delta function, $\delta(t)$, which is simply the impulse response of a dashpot with a constant coefficient. The latter is, of course, representative of a purely viscous medium.

The pulse shape function, $h(t)$, is identified as the time-dependent part of the solution in Eq. (18),

$$h(t) = \frac{\theta}{\xi_0} \left(1 + \frac{\theta}{\xi_0} t \right)^{-E/\theta}, \tag{20}$$

where the leading factor on the right has been included only to give $h(t)$ the dimensions of reciprocal time [the same as the delta function, $\delta(t)$]. The mean pulse amplitude is

$$\overline{a} = \chi_0 \frac{\xi_0}{\theta}, \tag{21}$$

and hence the time-dependence of the ensemble-averaged stress relaxation in Eq. (12) is

$$\begin{aligned} \overline{\sigma_{xz}(t)} &= \chi_0 \nu \overline{b} \left| \frac{dv_x(t)}{dz} \right| \otimes \left(1 + \frac{\theta}{\xi_0} t \right)^{-E/\theta} \mathrm{sgn}\left(\frac{dv_x(t)}{dz} \right) \\ &= \chi_0 \nu \overline{b} \frac{\xi_0}{\theta} \frac{dv_x(t)}{dz} \otimes \frac{\theta}{\xi_0} \left(1 + \frac{\theta}{\xi_0} t \right)^{-E/\theta}, \end{aligned} \tag{22}$$

where the leading coefficients on the right (i.e., $\chi_0 \nu \overline{b} \xi_0 / \theta$) are independent of the velocity gradient across the contact. Note that the signum function in Eq. (22) has the same arithmetic sign as that in Eq. (18).

Since the functional form on the right of Eq. (22) represents the average stress relaxation from individual microasperities sliding against one another, it holds for both translational and radial shearing. As can be seen from Eq. (22), an important property of the average stress is that it satisfies the principle of superposition, and hence is strictly linear, even though the strain-hardening Maxwell element representing an individual component of the random succession of stress pulses is nonlinear.

IX. TRANSLATIONAL (SHEAR) AND RADIAL (COMPRESSIONAL) GRAIN SHEARING

The internal stress relaxation arising from both translational and radial shearing is given by Eq. (22), with appropriate values for the various coefficients in the two cases. In particular, the grain-size dependence, which appears through the presence of the mean rate of events, ν, is different for the two types of shearing, as discussed in the Appendix. Incidentally, the translational and radial shearing processes may be thought of as being analogous to shear and bulk viscosity,[59] respectively, in a viscous fluid.

For convenience in discussing the coefficients in Eq. (22), the expressions for the stress associated with radial (compressional) and translational (shear) sliding are now written separately, as follows:

$$\sigma_{zz}(t) = \lambda_p h_p(t) \otimes \frac{dv_z(t)}{dz} \tag{23}$$

and

$$\sigma_{xz}(t) = \eta_s h_s(t) \otimes \frac{dv_x(t)}{dz}, \tag{24}$$

where the subscripts p and s identify the associated quantity with radial and translational shearing, respectively. The overbars denoting ensemble averaging have now been omitted for brevity. The $h_{p,s}(t)$ functions in Eqs. (23) and (24) are the material impulse response functions (MIRFs) for radial and translational shearing,

$$h_p(t) = t_p^{-1} \left(1 + \frac{t}{t_p} \right)^{-n}, \tag{25}$$

and

$$h_s(t) = t_s^{-1} \left(1 + \frac{t}{t_s} \right)^{-m}, \tag{26}$$

where, from inspection of Eq. (20), the stress-relaxation time constants are

$$t_p = \frac{\xi_{op}}{\theta_p}, \quad t_s = \frac{\xi_{os}}{\theta_s}, \tag{27}$$

and the material exponents are

$$n = \frac{E_p}{\theta_p}, \quad m = \frac{E_s}{\theta_s}. \tag{28}$$

Several of the scaling constants in the analysis conveniently collapse into just two coefficients, the radial and translational stress-relaxation coefficients, λ_p and η_s, in Eqs. (23) and (24). From comparison with Eq. (22),

$$\lambda_p = \chi_{op} \nu_p \overline{b_p} t_p \tag{29}$$

and

$$\eta_s = \chi_{os} \nu_s \overline{b_s} t_s. \tag{30}$$

The temporal convolutions for the radial and translational stresses in Eqs. (23) and (24), respectively, are identical to those introduced inductively in I and II. It is also apparent that the MIRFs in Eqs. (25) and (26) reduce to the inverse-time power laws used in I and II for times that are greater than the stress-relaxation time constants t_p, t_s. Since these time constants scale with the residual viscosity of the fluid in the film, ξ_0 [see Eq. (27)], which in granular materials appears to be negligible, it follows that for all time scales of interest the inverse-time power-law form for the MIRFs is an excellent approximation.

The time constants t_p, t_s and the exponents n, m defined in Eqs. (27) and (28) characterize a single, deterministic event, the sliding of one micro-asperity over another. Such events are the building blocks of both translational and radial stress relaxation. These constitutive events are physically indistinguishable in the two types of grain shearing, and therefore the following equalities are expected to hold:

$$t_p = t_s, \tag{31a}$$

$$m = n, \tag{31b}$$

and hence

$$h_p(t) \equiv h_s(t). \tag{32}$$

These equalities imply that the compressional and shear wave properties, that is, the two wave speeds and the two attenuations, are all causally connected. This linking imposes a strong constraint on the predicted wave properties, which will provide a demanding test of the grain-shearing theory.

Limited experimental evidence in support of the predicted equality between n and m has been presented in II. Further evidence indicating that $n = m$ is presented below in Figs. 6 and 7. However, in the interest of being explicit, the distinctions between t_p, t_s, between n,m, and between $h_p(t), h_s(t)$ are maintained throughout the remainder of the analysis. The identities in Eqs. (31) and (32) should be borne in mind, however, because they will be used later in evaluating the theoretical expressions for the wave speeds and attenuations.

It will turn out that the compressional and shear attenuations, respectively, scale in direct proportion to the material exponents n and m. According to Eqs. (28), these (dimensionless) exponents provide a relative measure of the conservative and dissipative forces in the microscopic sliding process represented by the nonlinear Maxwell element: n (or m) is the elastic modulus of the spring divided by the strain-hardening coefficient of the dashpot. As strain-hardening decreases $(n,m \to \infty)$, grain sliding is facilitated and attenuation rises, and as strain-hardening increases $(n,m \to 0)$ grains tend to lock together, little or no sliding can occur, and attenuation approaches zero. By comparison, the compressional and shear wave speeds are only weakly dependent on n and m, and hence are relatively insensitive to strain-hardening in the granular medium.

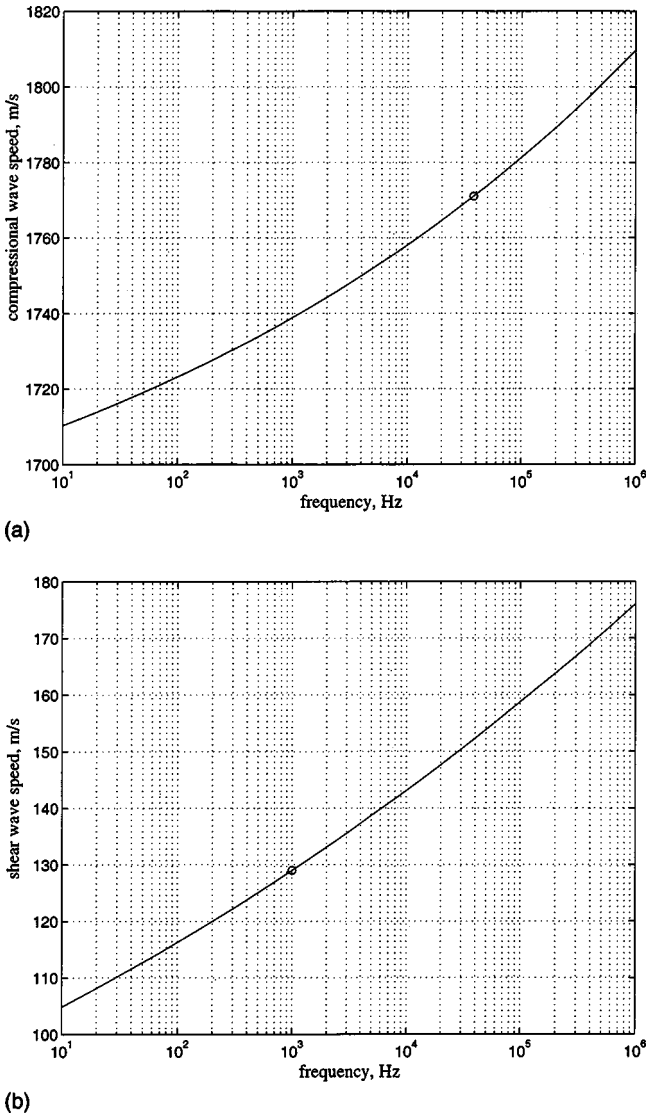

FIG. 6. Theoretical dispersion in the wave speeds for the SAX99 sediment. (a) The compressional wave and (b) the shear wave. The data points (○) used in determining the unknown coefficients fall on the theoretical curves.

X. GENERALIZED NAVIER–STOKES EQUATION

To establish the equation of motion, the granular medium is treated, macroscopically, as a homogeneous, fluid continuum, which, like a viscous fluid, is capable of supporting a shear ''flow.'' The continuum representation is valid for the wavelengths of interest, which are considerably longer than the size scale of the grain structure and the pore spaces in the material. The microscopic, randomly orientated grain boundaries may be thought of as being embedded in the continuum in such a way as to support the compressive and shear stresses described by Eqs. (23) and (24), respectively.

The assumption of homogeneity is obviously not consistent with Liu *et al.*'s[5] observations of force chains and the associated fluctuations in wave propagation, which are effects of inhomogeneity in the medium. By treating the material as (macroscopically) homogeneous, smoothed wave properties will be obtained, for instance, the average attenuation as a function of frequency. Once the average behavior has been established, the assumption of homogeneity could be relaxed in order to investigate interference between waves propagating along different force-chain pathways. This, however, is beyond the scope of the present article.

To set up the equation of motion, the full stress tensor, $\boldsymbol{\sigma}$, for the granular medium must be derived. The terms in this tensor relate stress to rate of strain at a point (x,y,z) in the three-dimensional medium. The argument is analogous to that for a homogeneous, isotropic, viscous fluid, as discussed by Morse and Ingard,[59] except that the stress, instead of being proportional to the velocity gradient, is in the form of the convolutions in Eqs. (23) and (24).

The tensor for the shear flow may be written as

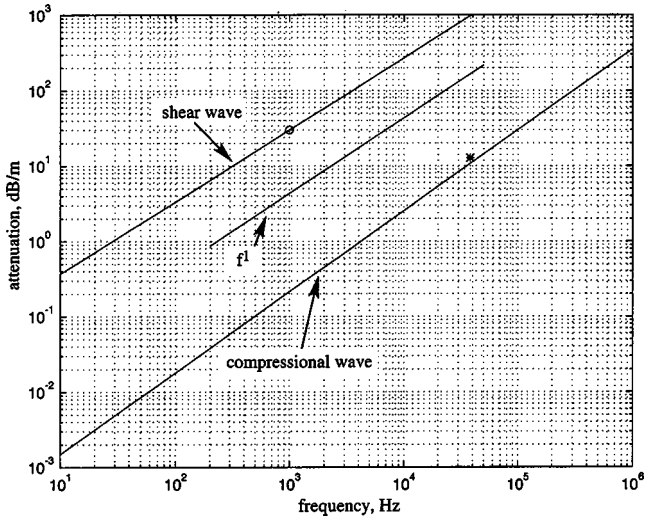

FIG. 7. Theoretical attenuation as a function of frequency for the SAX99 sediment. The shear wave data point (○), used in determining the unknown coefficients, falls on the theoretical curve. The compressional wave data point (*) lies about 2 dB/m above the theoretically predicted curve. The line labeled f^1 illustrates the slope of any attenuation that scales as the first power of frequency.

$$V=\begin{pmatrix} V_{xx} & V_{xy} & V_{xz} \\ V_{yx} & V_{yy} & V_{yz} \\ V_{zx} & V_{zy} & V_{zz} \end{pmatrix}, \tag{33}$$

where the diagonal components are

$$V_{ii}=\frac{\partial v_i}{\partial x_i}-\frac{1}{3}\operatorname{div}\mathbf{v}, \tag{34}$$

and the off-diagonal components $(i\neq j)$ are

$$V_{ij}=\frac{1}{2}\frac{\partial v_i}{\partial x_j}+\frac{1}{2}\frac{\partial v_j}{\partial x_i}=V_{ji}. \tag{35}$$

Equations (34) and (35) represent pure shear strains with no change in fluid content. Thus the tensor $\mathbf{V}$ in Eq. (33) is a measure of the rate at which one part of the medium slides past another at the point (x,y,z), excluding the effects of rotation and outflow of material from the unit volume around (x,y,z). The outflow has been removed by subtracting equal parts of the divergence of the velocity,

$$\operatorname{div}\mathbf{v}=\frac{\partial v_x}{\partial x}+\frac{\partial v_y}{\partial y}+\frac{\partial v_z}{\partial z}, \tag{36}$$

from the diagonal components of the tensor [Eq. (34)].

The stress tensor must include several components in addition to the term $-2\,\eta_s h_s(t)\otimes\mathbf{V}$ representing the translational shear between grains. [The factor of 2 is included here to maintain consistency with the simple case in Eq. (24).] Clearly, the hydrostatic pressure, including the acoustic pressure, p, must be added into the diagonal elements of $\boldsymbol{\sigma}$. A further term must also be included in the diagonal elements to account for the compressive stress associated with shearing along radials of the circle of contact. From Eq. (23), the appropriate term to be included is $-\lambda_p \operatorname{div} h_p(t)\otimes\mathbf{v}$, representing the stress relaxation arising from the rate of change of compression.

When the acoustic pressure, p, the radial compressive stress, and the translational shear stress are included, the stress tensor can be written as

$$\sigma=\{p-\lambda_p \operatorname{div}[h_p(t)\otimes\mathbf{v}]+\tfrac{2}{3}\eta_s \operatorname{div}[h_s(t)\otimes\mathbf{v}]\}\delta_{ij} - \eta_s\left[h_s(t)\otimes\left\{\frac{\partial v_i}{\partial x_j}+\frac{\partial v_j}{\partial x_i}\right\}\right], \tag{37}$$

where δ_{ij} is the Kronecker delta. The hydrostatic pressure has been neglected in Eq. (37) since it plays no part in the wave equations. If $h_p(t)$ and $h_s(t)$ were set equal to $\delta(t)$, then Eq. (37) would reduce identically to the stress tensor for a viscous fluid. This should be obvious, since the convolution of a delta function with any continuous function is the function itself. However, with the MIRFs taking the forms in Eqs. (25) and (26), the properties of the stress tensor in Eq. (37) are significantly different from those of the stress tensor for a viscous fluid.

If external forces such as gravity are neglected, the equations of motion may be written as

$$(\rho_0+\Delta)\frac{d\mathbf{v}}{dt}=(\rho_0+\Delta)\left[\frac{\partial\mathbf{v}}{\partial t}+(\mathbf{v}\cdot\operatorname{grad})\mathbf{v}\right]=-\nabla.\boldsymbol{\sigma}, \tag{38}$$

where ρ_0 is the bulk density of the material and Δ is the density fluctuation associated with the presence of a propagating wave. On linearizing this expression, the first-order, Navier–Stokes equation is obtained,

$$\rho_0\frac{\partial\mathbf{v}}{\partial t}=-\nabla\cdot\sigma=-\operatorname{grad}p+\lambda_p\ \operatorname{grad}\operatorname{div}[h_p(t)\otimes\mathbf{v}] + \tfrac{4}{3}\eta_s\ \operatorname{grad}\operatorname{div}[h_s(t)\otimes\mathbf{v}] - \eta_s\ \operatorname{curl}\ \operatorname{curl}\ [h_s(t)\otimes\mathbf{v}], \tag{39}$$

where the following relationships have been used:

$$(\nabla\mathbf{v})_{ij}=\frac{\partial v_j}{\partial x_i}, \tag{40}$$

$$(\mathbf{v}\nabla)_{ij}=\frac{\partial v_i}{\partial x_j}, \tag{41}$$

$$[\nabla\cdot(\mathbf{v}\nabla)]_j=[\operatorname{grad}(\operatorname{div}\mathbf{v})]_j, \tag{42}$$

and

$$[\nabla\cdot(\nabla\mathbf{v})]_j=[\operatorname{grad}(\operatorname{div}\mathbf{v})]_j-[\operatorname{curl}\ \operatorname{curl}\ \mathbf{v}]_j. \tag{43}$$

Equation (39) is the equation of motion appropriate to an unconsolidated granular medium in which radial (compressional) and translational (shear) stress relaxation is as given by Eqs. (23) and (24).

XI. WAVE EQUATIONS

The wave speeds and the associated attenuations are determined from the compressional and shear wave equations, which are developed below from the Navier–Stokes equation [Eq. (39)]. In addition, the equation of state is required, which for the granular medium is, to first order,

$$p=c_0^2\Delta, \tag{44}$$

where

$$c_0 = \sqrt{\frac{\kappa_0}{\rho_0}}. \tag{45}$$

Physically, c_0 is the compressional wave speed that would be observed in the absence of grain-to-grain stress relaxation, that is, if the granular medium were a suspension with no contact forces. Such a medium will be referred to as the ''equivalent suspension.'' The bulk modulus, κ_0, of the equivalent suspension is essentially defined through Eq. (45). Notice that in the limit of low frequency, because the rate of strain is zero, the three convolutions in Eq. (39) vanish and hence the wave properties of the granular medium are expected to be the same as those in the equivalent suspension.

The value of the wave speed, c_0, is not accessible through direct measurement. It can, however, be evaluated from Wood's equation,[60] that is, Eq. (45) with the bulk modulus, κ_0, and the bulk density, ρ_0, given by the weighed means

$$\frac{1}{\kappa_0} = N\frac{1}{\kappa_w} + (1-N)\frac{1}{\kappa_g} \tag{46}$$

and

$$\rho_0 = N\rho_w + (1+N)\rho_g. \tag{47}$$

In these expressions, N is the porosity of the granular medium, κ_w, κ_g are, respectively, the bulk moduli of seawater and of the mineral grains, and ρ_w, ρ_g are the corresponding densities. Since values for all these parameters are usually available, c_0 may be considered as known.

As an aside, N is governed by the packing arrangement of the grains. In a typical marine sediment, the sand grains form a random close-packing structure, which, by definition, is the tightest random packing arrangement possible. In a homogeneous material, the random packing is expected to hold at all depths in the sediment, from which it follows that N should be invariant with depth (at least, until the overburden pressure becomes so great as to crush the asperities on the grains). Data exhibiting the depth-invariance of N immediately beneath the sediment interface have been presented by Richardson and Briggs[61] and Richardson.[62] If N is invariant with depth, it follows from Eqs. (46) and (47) that the bulk modulus and density must behave similarly.

Returning to the derivation of the wave equations, conservation of mass requires that

$$\frac{\partial \Delta}{\partial t} + \rho_0 \nabla \cdot \mathbf{v} = 0, \tag{48}$$

which, when combined with Eq. (44), yields

$$\frac{1}{c_0^2}\frac{\partial p}{\partial t} + \rho_0 \nabla \cdot \mathbf{v} = 0. \tag{49}$$

On eliminating the acoustic pressure, p, from Eqs. (39) and (49), by differentiating the former with respect to time, the following equation for the velocity $\mathbf{v}$ is obtained:

$$\rho_0 \frac{\partial^2 \mathbf{v}}{\partial t^2} = \kappa \,\mathrm{grad}\,\mathrm{div}\,\mathbf{v} + \lambda_p \;\mathrm{grad}\;\mathrm{div}\frac{\partial}{\partial t}[h_p(t)\otimes \mathbf{v}] + \frac{4}{3}\eta_s \,\mathrm{grad}\,\mathrm{div}\frac{\partial}{\partial t}[h_s(t)\otimes \mathbf{v}] - \eta_s \;\mathrm{curl}\;\mathrm{curl}\frac{\partial}{\partial t}[h_s(t)\otimes \mathbf{v}]. \tag{50}$$

According to Helmholtz's theorem,[63] any vector field, $\mathbf{v}$, can be expressed as the sum of the gradient of a scalar potential, ψ, and the curl of a zero-divergence vector potential, $\mathbf{A}$,

$$\mathbf{v} = \mathrm{grad}\,\psi + \mathrm{curl}\;\mathbf{A}; \quad \mathrm{div}\,\mathbf{A} = 0. \tag{51}$$

On substituting the first of these expressions into Eq. (49) and performing a straightforward separation of terms, the following two equations are obtained:

$$\nabla^2\psi - \frac{1}{c_0^2}\frac{\partial^2\psi}{\partial t^2} + \frac{\lambda_p}{\rho_0 c_0^2}\frac{\partial}{\partial t}\nabla^2[h_p(t)\otimes\psi] + \frac{(4/3)\eta_s}{\rho_0 c_0^2}\frac{\partial}{\partial t}\nabla^2[h_s(t)\otimes\psi] = 0 \tag{52}$$

and

$$\frac{\eta_s}{\rho_0}\nabla^2[h_s(t)\otimes\mathbf{A}] - \frac{\partial \mathbf{A}}{\partial t} = 0, \tag{53}$$

where ∇^2 is the Laplacian, and the identities curl grad $\psi = 0$, div curl $\mathbf{A} = 0$, and curl curl $\mathbf{A} = -\nabla^2\mathbf{A}$ have been used. Equations (52) and (53), representing, respectively, the propagation of compressional and shear disturbances in an unconsolidated granular medium, were stated in II but without the formal derivation given above. A minor error in II in the compressional-wave equation has been corrected in Eq. (52).

At first glance, the presence of the first derivative with respect to time might suggest that Eq. (53) for shear disturbances is diffusionlike rather than wavelike in character. This would, in fact, be the case if $h_s(t)$ were a delta function, representative of viscous dissipation. According to Eq. (53), shear disturbances in a viscous fluid are evanescent, decaying away exponentially in time and space, which is why it is said that shear is not supported by a fluid. When $h_s(t)$ is not a delta function, however, but takes the form in Eq. (26), solutions of Eq. (53) exist which represent propagating shear waves, as discussed in II. Physically, the rigidity introduced by strain-hardening during translational shearing is the factor responsible for the predicted shear wave.

XII. WAVE SPEEDS AND ATTENUATIONS

Expressions for the speed and attenuation of the compressional and shear wave are obtained by Fourier transforming the wave equations in Eqs. (52) and (53) with respect to time. This yields the reduced wave equations

$$\nabla^2\Psi + \frac{\omega^2/c_0^2}{\left[1 + \frac{j\omega}{\rho_0 c_0^2}\{\lambda_p H_p(j\omega) + (4/3)\eta_s H_s(j\omega)\}\right]}\Psi = 0 \tag{54}$$

and

$$\nabla^2\hat{\mathbf{A}}+\frac{\omega^2\rho_0}{j\omega\eta_s H_s(j\omega)}\hat{\mathbf{A}}=0, \tag{55}$$

where $(\Psi,\hat{\mathbf{A}},H_p,H_s)$ are the Fourier transforms with respect to time of $(\psi,\mathbf{A},h_p,h_s)$, ω is angular frequency, and $j=\sqrt{-1}$. Note that the temporal convolutions in Eqs. (52) and (53), representing compressive and shear stress relaxation, appear as products in the frequency domain [Eqs. (54) and (55)]. From the plane-wave solution of Eq. (54), the phase speed, c_p, loss tangent, β_p, and attenuation coefficient, α_p, of the compressional wave can immediately be written as

$$\frac{1}{c_p}=\frac{1}{c_0}\mathrm{Re}\left[1+\frac{j\omega}{\rho_0 c_0^2}\{\lambda_p H_p(j\omega)+(4/3)\eta_s H_s(j\omega)\}\right]^{-1/2}, \tag{56a}$$

$$\beta_p=-\frac{c_p}{c_0}\mathrm{Im}\left[1+\frac{j\omega}{\rho_0 c_0^2}\{\lambda_p H_p(j\omega)+(4/3)\eta_s H_s(j\omega)\}\right]^{-1/2}, \tag{56b}$$

and

$$\alpha_p=\frac{\omega\beta_p}{c_p}. \tag{56c}$$

Similarly for the shear wave, the phase speed, c_s, the loss tangent, β_s, and the attenuation coefficient, α_s, are, from the plane-wave solution of Eq. (55),

$$\frac{1}{c_s}=\sqrt{\frac{\rho_0}{\eta_s}}\mathrm{Re}[j\omega H_s(j\omega)]^{-1/2}, \tag{57a}$$

$$\beta_s=-c_s\sqrt{\frac{\rho_0}{\eta_s}}\mathrm{Im}[j\omega H_s(j\omega)]^{-1/2}, \tag{57b}$$

and

$$\alpha_s=\frac{\omega\beta_s}{c_s}. \tag{57c}$$

Incidentally, the loss tangents can be expressed as $\beta=1/2Q$, where Q is the quality factor of the medium. [N.B., The coefficients in Eqs. (56c) and (57c) give the attenuation of a planar pressure wave in nepers/m; they should be doubled to give the attenuation of intensity.]

The temporal Fourier transforms of the MIRFs in Eqs. (25) and (26) are, respectively,

$$H_p(j\omega)=(j\omega t_p)^{n-1}e^{j\omega t_p}\Gamma(1-n,j\omega t_p)\approx\frac{\Gamma(1-n)}{(j\omega t_p)^{1-n}} \tag{58}$$

and

$$H_s(j\omega)=(j\omega t_s)^{m-1}e^{j\omega t_p}\Gamma(1-m,j\omega t_s)\approx\frac{\Gamma(1-m)}{(j\omega t_s)^{1-m}}, \tag{59}$$

where ω is angular frequency and $\Gamma(...,....)$ is the complement of the incomplete gamma function. The approximations in Eqs. (58) and (59) hold at all frequencies for which $\omega t_{p,s}\ll 1$, conditions which are satisfied in unconsolidated, saturated marine sediments, where viscous effects, represented by the time constants t_p and t_s, appear to be negligible.

When Eqs. (58) and (59) are substituted into the expressions for the wave speeds and loss tangents, Eqs. (56) and (57) become

$$\frac{1}{c_p}=\frac{1}{c_0}\mathrm{Re}\left[1+\frac{\mu_p}{\rho_0 c_0^2}(j\omega t_p)^n+\frac{4}{3}\frac{\mu_s}{\rho_0 c_0^2}(j\omega t_s)^m\right]^{-1/2}, \tag{60a}$$

$$\beta_p=-\frac{c_p}{c_0}\mathrm{Im}\left[1+\frac{\mu_p}{\rho_0 c_0^2}(j\omega t_p)^n+\frac{4}{3}\frac{\mu_s}{\rho_0 c_0^2}(j\omega t_s)^m\right]^{-1/2}, \tag{60b}$$

$$\alpha_p=-\frac{\omega}{c_0}\mathrm{Im}\left[1+\frac{\mu_p}{\rho_0 c_0^2}(j\omega t_p)^n+\frac{4}{3}\frac{\mu_s}{\rho_0 c_0^2}(j\omega t_s)^m\right]^{-1/2}, \tag{60c}$$

and

$$\frac{1}{c_s}=\frac{1}{c_0}\mathrm{Re}\left[\frac{\mu_s}{\rho_0 c_0^2}(j\omega t_s)^m\right]^{-1/2}=\frac{1}{c_0}\sqrt{\frac{\rho_0 c_0^2}{\mu_s}}|\omega t_s|^{-m/2}\cos\left(\frac{m\pi}{4}\right), \tag{61a}$$

$$\beta_s=-\frac{c_s}{c_0}\mathrm{Im}\left[\frac{\mu_s}{\rho_0 c_0^2}(j\omega t_s)^m\right]^{-1/2}=\mathrm{sgn}(\omega)\tan\left(\frac{m\pi}{4}\right), \tag{61b}$$

$$\alpha_s=\frac{|\omega|}{c_0}\sqrt{\frac{\rho_0 c_0^2}{\mu_s}}|\omega t_s|^{-m/2}\sin\left(\frac{m\pi}{4}\right). \tag{61c}$$

The parameters μ_p,μ_s in these expressions are, respectively, radial and translational stress-relaxation moduli, which are related to the stress-relaxation coefficients λ_p and η_s as follows:

$$\mu_p=\frac{\lambda_p}{t_p}\Gamma(1-n) \tag{62a}$$

and

$$\mu_s=\frac{\eta}{t_s}\Gamma(1-m). \tag{62b}$$

It is evident from Eq. (60a) that one effect of these moduli is to raise the compressional wave speed of the sediment above the value c_0 of the equivalent suspension.

The expressions for the wave speeds and attenuations in Eqs. (60) and (61) can be simplified, first by adopting the predicted equalities in Eq. (31), and second by amalgamating the stress-relaxation moduli with the time constant $t_0\equiv t_p=t_s$. Then, the speed, loss tangent, and attenuation of the compressional wave can be written as

$$\frac{1}{c_p}=\frac{1}{c_0}\mathrm{Re}\left[1+\frac{3\gamma_p+4\gamma_s}{3\rho_0 c_0^2}(j\omega T)^n\right]^{-1/2}, \tag{63a}$$

$$\beta_p=-\frac{c_p}{c_0}\mathrm{Im}\left[1+\frac{3\gamma_p+4\gamma_s}{3\rho_0 c_0^2}(j\omega T)^n\right]^{-1/2}, \tag{63b}$$

$$\alpha_p = -\frac{\omega}{c_0}\,\mathrm{Im}\left[1+\frac{3\gamma_p+4\gamma_s}{3\rho_0 c_0^2}(j\omega T)^n\right]^{-1/2}, \tag{63c}$$

and for the shear wave,

$$\frac{1}{c_s} = \frac{1}{c_0}\sqrt{\frac{\rho_0 c_0^2}{\gamma_s}}\,|\omega T|^{-n/2}\cos\left(\frac{n\pi}{4}\right), \tag{64a}$$

$$\beta_s = \mathrm{sgn}(\omega)\tan\left(\frac{n\pi}{4}\right), \tag{64b}$$

$$\alpha_s = \frac{|\omega|}{c_0}\sqrt{\frac{\rho_0 c_0^2}{\gamma_s}}\,|\omega T|^{-n/2}\sin\left(\frac{n\pi}{4}\right). \tag{64c}$$

In these expressions, γ_p and γ_s are, respectively, compressional and shear rigidity coefficients,

$$\gamma_p = \mu_p\left(\frac{t_0}{T}\right)^n \tag{65a}$$

and

$$\gamma_s = \mu_s\left(\frac{t_0}{T}\right)^n, \tag{65b}$$

where T is an arbitrary time that has been introduced solely to keep terms raised to the fractional power of n dimensionless. It should be clear that the expressions in Eqs. (63) and (64) are independent of the value of T, which is conveniently taken to be $T=1$ s.

XIII. EVALUATION OF THE GRAIN-SHEARING COEFFICIENTS

Equations (63) and (64) are our final, exact expressions for the wave speeds and attenuations in the granular medium. It can be seen that, besides the mechanical properties of the two constituent materials and the porosity of the granular system, all of which may be taken as known, these expressions involve just three unknown coefficients γ_p, γ_s, and n, which must be determined from data. Two of the coefficients, γ_p and γ_s, respectively, represent the ensemble-averaged stresses associated with radial and translational sliding. The third coefficient, the material exponent n, characterizes the deterministic interaction between individual micro-asperities at the contacts between grains.

To evaluate these coefficients, only three of the expressions for the wave properties are required, the two wave speeds [Eqs. (63a) and (64a)] and the shear attenuation [Eq. (64c)]. The fourth expression, for the compressional attenuation, can then be evaluated to yield a prediction, which may be tested against data.

It is assumed that measurements of the compressional wave speed and attenuation are available at a spot frequency, f_p, and similarly for the shear wave at spot frequency f_s. By forming the product of the shear wave speed and attenuation from Eqs. (64a) and (64c), an expression is obtained which involves only n,

$$c_s(\omega_s)\,\alpha_s(\omega_s) = |\omega_s|\tan\frac{n\pi}{4}, \tag{66}$$

where $\omega_s = 2\pi f_s$. It follows that n is uniquely specified as

$$n = \frac{4}{\pi}\tan^{-1}\left\{\frac{c_s(\omega_s)\,\alpha_s(\omega_s)}{|\omega_s|}\right\}. \tag{67}$$

Note that α_s in these expressions is in nepers/m, which is obtained by dividing dB/m by $20\log_{10}(e) = 8.686$.

The coefficient γ_s may be obtained either from the speed or attenuation of the shear wave. Taking the wave speed in Eq. (64a), it follows that

$$\gamma_s = \frac{\rho_0 c_s^2(\omega_s)}{|\omega_s|^n}\cos^2\frac{n\pi}{4}, \tag{68}$$

where we have set $T=1$ s. Equation (68) specifies γ_s uniquely. The remaining parameter, γ_p, may now be evaluated in a straightforward manner from Eq. (63a) for the compressional wave speed. It is easier to do this numerically using a simple algorithm, rather than develop a clumsy analytical solution.

Once γ_p, γ_s, and n have been evaluated, the expressions in Eqs. (63) and (64) provide the full frequency dependence for the wave speeds and attenuations. At present, a difficulty in testing the theory is that few data sets are available in the literature which fully characterize a sediment. The required data are: the porosity, N, the shear wave speed and attenuation at frequency f_s, and the compressional wave speed and attenuation at frequency f_p. Often, four out of these five parameters are reported, but usually the attenuation of the shear wave is not available.

Recently, however, as part of an O.N.R. research initiative designated SAX99, a quartz sand sediment in the northeastern Gulf of Mexico off the Florida Panhandle was intensively investigated. Preliminary data from SAX99, including all five parameters required for the test, have been reported by Richardson *et al.*[64] The values are: $N=0.39$ (from electrical conductivity measurements); $c_p = 1771$ m/s and $\alpha_p = 12.7$ dB/m, both at $f_p = 38$ kHz; $c_s = 129$ m/s and $\alpha_s = 30$ dB/m, both at $f_s = 1$ kHz. The temperature of the pore water was 22 °C, giving $\rho_w = 1024.2$ g/m^3, $\kappa_w = 2.388\times10^9$ Pa, and $c_w = 1527$ m/s. For quartz, $\rho_g = 2650$ kg/m^3 and $\kappa_g = 3.36\times10^{10}$ Pa. Thus the sound speed in the equivalent suspension is $c_0 = 1653.4$ m/s and the bulk density of the sediment is $\rho_0 = 2015.9$ kg/m^3. These data (excluding α_p) yield: $n = 0.090\,14$; $\gamma_p = 2.48\times10^8$ Pa; and $\gamma_s = 1.517\times10^7$ Pa.

Figures 6(a) and (b) show the compressional and shear wave speeds as functions of frequency, from Eqs. (63a) and (64a), respectively, for the SAX99 site. The small circles, lying precisely on the theoretical lines, are two of the data points that were used in determining the coefficients. For the same site, Fig. 7 shows the compressional and shear wave attenuations as functions of frequency, from Eqs. (63c) and (64c), respectively. The small circle in this figure, lying precisely on the theoretical curve for the shear attenuation, is the third data point that was used in evaluating the coefficients.

The asterisk in Fig. 7, the measured compressional attenuation, was not used in evaluating the coefficients. At a frequency of 38 kHz, the theoretically predicted curve lies at 10.7 dB/m, about 16% (2 dB/m) below the data point represented by the asterisk. In view of the fact that the compressional and shear attenuations differ by over two orders of

magnitude, the correspondence between the predicted compressional attenuation and the data in Fig. 7 is considered to be very satisfactory. It is only fair to point out, however, that the values of the SAX99 wave properties used to obtain the prediction are preliminary and may be revised as the data are examined in greater detail. This serves to emphasize the need for more complete data sets on the wave properties of sediments.

In performing a test like that illustrated in Fig. 7 it is important, first, to take proper account of the temperature of the pore fluid[65] and, second, to use the best available measure of porosity. Both affect the computed value of c_0, which in turn influences the predicted value of α_p. To illustrate the effect of the porosity, suppose that N is raised by 1% from 0.39, as in the above calculation, to 0.40. Then, with the same input wave properties, the predicted compressional attenuation is $\alpha_p = 11.65$ dB/m, an increase of about 1 dB/m or approximately 10%. In sandy sediments, the wave properties are highly sensitive to the porosity.

XIV. APPROXIMATIONS

Although the exact expressions for the wave speeds and attenuations are easy to compute, the functional trends are not immediately apparent from Eqs. (63) and (64). Approximations for these expressions are derived in I and II, from which the various dependencies are more evident. Just a summary of the results is given below.

By expanding Eqs. (63) and (64) in Taylor series to first order in the small parameter n, the following results are obtained:

$$c_p \approx c_0 \sqrt{1+\Gamma_p+\frac{4}{3}\Gamma_s}\left[1+\frac{2\beta_p}{\pi}\ln|\omega T|\right], \tag{69a}$$

$$\beta_p \approx \frac{n\pi\Gamma_p}{4(1+\Gamma_p)}\,\mathrm{sgn}(\omega), \tag{69b}$$

$$\alpha_p \approx \frac{n\pi|\omega|\Gamma_p}{4c_0(1+\Gamma_p)^{3/2}}, \tag{69c}$$

and

$$c_s \approx c_0\sqrt{\Gamma_s}\left[1+\frac{2\beta_s}{\pi}\ln|\omega T|\right], \tag{70a}$$

$$\beta_s \approx \frac{n\pi}{4}\,\mathrm{sgn}(\omega), \tag{70b}$$

$$\alpha_s \approx \frac{n\pi|\omega|}{4c_0\sqrt{\Gamma_s}}. \tag{70c}$$

For brevity, normalized stress-relaxation moduli have been introduced in these expressions,

$$\Gamma_p = \frac{\gamma_p}{\rho_0 c_0^2} \tag{71a}$$

and

$$\Gamma_s = \frac{\gamma_s}{\rho_0 c_0^2}. \tag{71b}$$

It is clear from the approximations in Eqs. (69c) and (70c) that the predicted attenuation of the compressional and shear wave both scale as the first power of frequency. This is confirmed in Fig. 7, where the exact expressions for the attenuations can be seen to follow an essentially linear scaling with frequency over several decades.

The approximate wave speeds in Eqs. (69a) and (70a) show logarithmic dispersion, the form of which is identical with that found by several other authors[31–36] for a wave whose attenuation scales as the first power of frequency. The dispersion scales with the loss tangent, β, or inversely as the Q. Thus the level of dispersion in the shear wave is significantly higher than that in the compressional wave. For the SAX99 site, $\beta_p \approx 0.01$ and $\beta_s \approx 0.07$, yielding dispersion of approximately 1.5% and 10.3% per decade of frequency in the compressional and shear wave, respectively.

At 1.5% per decade, the predicted dispersion in the compressional wave is comparable with the experimental value obtained by Wingham[39] for a medium sand. It is also similar to the dispersion in saturated glass beads measured by Hovem and Ingram[66] in the frequency range between 15 and 300 kHz. The overall trend of their data is logarithmic with a slope of approximately 1.6% per decade. The Biot curve that they attempted to fit to the data (their Fig. 3) seems to have a slope that is too shallow and a magnitude that overestimates the sound speed at the lower frequencies.

An interesting feature of the logarithmic approximations for the wave speeds is that, in the limit of low frequency, the expressions in Eqs. (69a) and (70a) diverge to negative infinity. In contrast, the exact expressions in Eqs. (63a) and (64a) are well-behaved throughout the entire range of frequency. At zero frequency, the exact wave speeds reduce to $c_p = c_0$ and $c_s = 0$, and both attenuations are zero. These are just the properties of the equivalent suspension in which there are no grain-to-grain stresses. As mentioned earlier, this limiting behavior is to be expected because the intergranular shearing depends on the rate of strain, which is zero in the limit of low frequency.

Although the logarithmic approximations and the exact expressions for the wave speeds diverge at low frequency, there is nevertheless a wide frequency range in which Eqs. (69) and (70) accurately approximate the exact forms in Eqs. (63) and (64). The logarithmic trend in the exact wave speeds is evident in Figs. 6(a) and (b). A comparative discussion of the exact versus approximate forms has been given by Buckingham.[67]

XV. "FRAME" ELASTICITY

Hamilton[68] developed an empirical model of wave propagation in unconsolidated granular materials in which the medium is treated as a Hookean elastic solid. In his model, the compressional and shear wave speeds are given by the familiar expressions for an isotropic elastic medium,

$$\hat{c}_p = \sqrt{\frac{\hat{K}+\frac{4}{3}\hat{\mu}}{\hat{\rho}_0}} \tag{72}$$

and

$$\hat{c}_s = \sqrt{\frac{\hat{\mu}}{\hat{\rho}_0}}, \tag{73}$$

where the tilde denotes one of Hamilton's elastic parameters. The bulk modulus of the saturated granular system is $\hat{\kappa}$, the bulk density is $\hat{\rho}_0$, and the shear modulus is $\hat{\mu}$. Hamilton[68] extended the elastic model to include dissipation by making $\hat{\mu}$ and the second Lamé constant, $\hat{\lambda} = \hat{\kappa} - 2/3\hat{\mu}$, complex. This he referred to as a viscoelastic model. He let the imaginary parts of the Lamé coefficients be independent of frequency simply because this yielded attenuations that scaled as the first power of frequency.

A recurring difficulty with the viscoelastic model, as discussed by Hamilton,[68] is the evaluation of the system bulk modulus, $\hat{\kappa}$. As others had done before him, Hamilton assumed implicitly that the unconsolidated granular medium possesses a skeletal elastic ''frame,'' and that one component of $\hat{\kappa}$ is the frame bulk modulus, $\hat{\kappa}_f$. He was then faced with the problem of determining $\hat{\kappa}_f$. His solution was to fit Gassman's equation[47] to available wave data, from which he inferred a value for the frame bulk modulus. With a judicious choice of the remaining elastic parameters, he then found that the equations of the elastic model could be made to fit measured data rather well.

The equations of Hamilton's elastic model may be interpreted in terms of the lowest-order approximations for the wave speeds predicted by the grain-shearing theory. Thus if the first-order, logarithmic terms representing dispersion are neglected, the wave speeds in Eqs. (69a) and (70a) reduce to the zero-order forms

$$c_p \approx \sqrt{\frac{\kappa_0 + \gamma_p + \frac{4}{3}\gamma_s}{\rho_0}} \tag{74}$$

and

$$c_s \approx \sqrt{\frac{\gamma_s}{\rho_0}}. \tag{75}$$

These expressions have exactly the same structure as those in Eqs. (72) and (73) for the wave speeds in an elastic medium.

Obviously, the bulk densities in the two models are identical: $\rho_0 = \hat{\rho}_0$. By comparing the expressions for the shear speed, Hamilton's shear rigidity modulus, $\hat{\mu}$, may be identified directly with γ_s, the shear rigidity conferred by grain-to-grain translation, and, from the compressional speeds, Hamilton's bulk modulus for the system equates as follows:

$$\hat{\kappa} = \kappa_0 + \gamma_p, \tag{76}$$

where γ_p is the compressional rigidity coefficient of the grain-shearing theory. According to Eqs. (74) and (76), two factors are responsible for raising the compressional speed in the granular medium above that in the equivalent suspension. The larger of the two is the rigidity due to radial (compressive) shearing, represented by γ_p. An order of magnitude smaller is the rigidity introduced by translational shearing and represented by γ_s. The frame bulk modulus may be interpreted in terms of the former, that is, the rigidity due to intergranular shearing under compression.

The Gassmann model[47] yields the bulk modulus of the system in terms of the ''frame'' bulk modulus, $\hat{\kappa}_f$, and the bulk modulus of the equivalent suspension, κ_0,

$$\hat{\kappa} = \kappa_0 + \frac{\hat{\kappa}_f(\kappa_g - \kappa_0)^2}{(\kappa_g^2 - \hat{\kappa}_f\kappa_0)}. \tag{77}$$

This expression is not as formulated by Gassmann, but is readily derived from his original with a little algebra. Apart from Hamilton,[68] several authors have examined Gassmann's equation, including White and Sengbush[69] and Wyllie *et al.*[40] As pointed out by Hamilton,[68] when the bulk modulus of the frame, $\hat{\kappa}_f$, is zero, the Gassmann equation reduces to Wood's equation, that is, $\hat{\kappa} = \kappa_0$, and when the porosity, N, is zero, corresponding to an elastic solid, $\hat{\kappa} = \kappa_0 = \kappa_g$. Hamilton[68] also states, erroneously, that, when N is zero, the solution of Eq. (77) for the frame bulk modulus is $\hat{\kappa}_f = \kappa_g$. Actually, $\hat{\kappa}_f$ is indeterminate from Gassmann's equation when $N = 0$. It follows that the four points on the ordinate in Hamilton's[68] Fig. 2 are invalid.

From inspection of Eqs. (76) and (77), γ_p of the grain-shearing theory may be linked to the elastic frame bulk modulus $\hat{\kappa}_f$ as follows:

$$\gamma_p = \frac{\hat{\kappa}_f(\kappa_g - \kappa_0)^2}{(\kappa_g^2 - \hat{\kappa}_f\kappa_0)}. \tag{78}$$

This equation may be inverted to yield

$$\hat{\kappa}_f = \frac{\gamma_p\kappa_g^2}{(\kappa_0 - \kappa_g)^2 + \gamma_p\kappa_0}. \tag{79}$$

Thus an ''effective'' elastic frame with a bulk modulus, $\hat{\kappa}_f$, as given by Eq. (79), is equivalent, at this lowest order of approximation, to the compressional rigidity that arises from radial (compressional) shearing at the grain contacts.

Of course, by assuming an elastic frame at the outset, many of the wave properties will be lost. For instance, as Hamilton[68] makes clear, his viscoelastic model is purely empirical and does not account for subtleties such as frequency dispersion in the wave speeds. Nor does it identify any correlations between the wave speeds and attenuations, but leaves them unconstrained. There are four free parameters in the viscoelastic model, the bulk modulus, the shear modulus, and the imaginary parts of the two Lamé coefficients. These can be individually adjusted to fit any wave-data set in which the two wave speeds are essentially independent of frequency and the two attenuations scale as the first power of frequency. In contrast, in the grain-shearing analysis, the wave properties are causally connected and hence heavily constrained.

On a historical note, in addition to recognizing that a saturated sediment exhibits shear rigidity, which supports the transmission of a transverse wave, Hamilton[68] was also aware that the speed of the compressional wave is greater than that predicted by Wood's equation. He attributed the enhanced compressional wave speed to two factors, ''the presence of both (shear) rigidity and a frame bulk modulus.'' His viscoelastic model [Eqs. (72) and (73)] embodies these ideas, and, although he did not specify physical mechanisms, he recognized that the shear rigidity and the frame bulk

modulus both originate in grain-to-grain interactions. This is exactly as has been argued above, where the frame bulk modulus is identified with the rigidity arising from radial (compressional) sliding, and the shear rigidity with translational sliding. Hamilton's[68] remarkable insights, expressed some three decades ago, provide an excellent foundation for understanding wave propagation in granular media.

XVI. CONCLUDING REMARKS

The linear theory of wave propagation in unconsolidated granular media developed in this paper is based on two distinct types of grain-to-grain interaction, translational and radial shearing, which occur during the passage of a wave through the medium. Both types of shearing are treated as a random stick-slip process consisting of a sequence of discrete ''micro-events.'' Each such event involves one microasperity slipping against another to produce a deterministic pulse of stress, a process which occurs as the medium relaxes after the application of a dynamic strain.

The mean stress, which governs the wave properties, is derived as an ensemble average of the random succession of stress-relaxation pulses. This average takes the form of a temporal convolution between the probability that a slip is triggered and the pulse shape function for a single stress-relaxation event. The probability density function is proportional to the velocity gradient normal to a grain contact, or equivalently, to the rate of strain across the boundary. The pulse shape function is established from a simple model of strain-hardening, which is based on the physics of the very thin film of pore fluid separating mineral grains. The resultant pulse shape function, or material impulse response function (MIRF), is essentially an inverse-time fractional power law.

With the stresses due to intergranular interactions specified as temporal convolutions, the Navier–Stokes equation is derived from the full stress tensor for the granular medium. A standard separation of the Navier–Stokes equation yields two wave equations, one for compressional and the other for shear disturbances. Both are true wave equations, even though the medium is treated as a fluid in the sense of possessing no skeletal elastic frame. By Fourier transforming these equations into the frequency domain, simple algebraic expressions for the wave speeds and attenuations are developed. These expressions depend explicitly on frequency and the porosity of the sediment.

The theoretical expressions for the compressional and shear attenuation both scale essentially in proportion to the first power of frequency. They compare very favorably with the published frequency dependence of compressional and shear wave attenuation data over many decades of frequency. The wave speeds are predicted to exhibit weak, near-logarithmic dispersion, the level of which scales with the loss tangent. Thus dispersion in the shear wave is estimated to be significantly higher than that in the compressional wave. These logarithmic expressions for the wave speeds are consistent with the Kramers–Kronig relationships, which lead to an identical form of logarithmic dispersion for any wave exhibiting an attenuation that scales with the first power of frequency, regardless of the physical mechanism responsible for the attenuation.

ACKNOWLEDGMENTS

I wish to thank Dr. Michael Richardson, N.R.L., Stennis Space Center, for very generously making many of his unpublished data sets available to me. This work was supported by the Ocean Acoustics Code (Dr. J. Simmen), Office of Naval Research under Grant No. N00014-93-1-0054.

APPENDIX: WAVE PROPERTIES VERSUS GRAIN SIZE AND DEPTH IN THE SEDIMENT

The coefficients γ_p and γ_s scale with the mean rate, $\nu_{p,s}$, of stress-relaxation events in the interval $[0,T]$. These mean rates are proportional to the total number of asperities available for sliding. Thus for translational shearing, ν_s is proportional to the area of the surface of contact, and for radial shearing ν_p is proportional to the radius of the circle of contact.

The Hertz theory[70] of identical elastic spheres pressed together by a force F gives the radius of the circle of contact as

$$a = \sqrt[3]{\frac{3}{8} F \frac{(1-\theta_g^2)}{E_g} u_g}, \tag{A1}$$

where u_g is the diameter of the spheres and (E_g, θ_g) are Young's modulus and Poisson's ratio for the material comprising the spheres. Equation (A1) applies to spheres that are frictionless. If the spheres are identified with mineral grains, then F scales with depth, d, in the sediment, and it follows that

$$\nu_p \propto (u_g d)^{1/3} \tag{A2}$$

and

$$\nu_s \propto (u_g d)^{2/3}. \tag{A3}$$

Thus according to the Hertz theory, $\gamma_{p,s}$ depend on grain size and depth as follows:

$$\gamma_p = \gamma_{op} \left(\frac{u_g d}{u_0 d_0} \right)^{1/3} \tag{A4}$$

and

$$\gamma_s = \gamma_{os} \left(\frac{u_g d}{u_0 d_0} \right)^{2/3}, \tag{A5}$$

where γ_{op}, γ_{os} are scaling constants, and $u_0 = 1000\,\mu$m, $d_0 = 0.3$ m, are normalizing factors, introduced solely to keep the bracketed terms dimensionless.

When the expression for γ_s in Eq. (A5) is substituted into Eq. (75), the speed of the shear wave is found to be

$$c_s \approx \left(\frac{u_g d}{u_0 d_0} \right)^{1/3} \sqrt{\frac{\gamma_{os}}{\rho_0}}. \tag{A6}$$

Figure 5 in II compares this expression, plotted as a function of grain size, with data on the shear wave speed as a function of grain size. The data show some scatter but straddle Eq. (A6) over three decades of grain size. The variation of c_s as the one-third power of depth, d, has been observed in sands

by Richardson *et al.*,[71] and Hamilton[72] proposed a similar power-law scaling, of the form $c_s \propto d^{0.28}$, based on a curve fit to data for sands.

The speed of the compressional wave varies relatively slowly with grain size and depth in the sediment. As predicted by Eqs. (74) and (A4), the grain-size dependence of c_p compares favorably with data over three decades of grain size (see Fig. 8 in I). The predicted depth dependence of c_p appears to be consistent with data from the West Florida Sand Sheet reported by Richardson and Briggs.[61]

It should be borne in mind when evaluating the grain-size dependence of the wave speeds and attenuations that the expressions involve ρ_0 and c_0, both of which are functions of the porosity, and the porosity varies with the grain size. In I, a relationship between porosity and grain size was proposed, based on a randomly packed, rough-grain model of the sediment,

$$N = 1 - P\left\{\frac{u_g + 2D}{u_g + 4D}\right\}^3, \tag{A7}$$

where $P = 0.63$ is the packing factor of a random, close-packing of smooth spheres, and D is the r.m.s. grain roughness. When $D = 0$, Eq. (A7) yields $N = 0.37$, which is the correct porosity for a random packing of smooth spheres.[73]

In sediments, it is well known that N is not single-valued in the grain size, one reason being that the grains of a given size may show different degrees of roughness. For most sands, D lies somewhere between 0 and 10 μm. If D is treated as a parameter, any of the wave properties, say the approximate expression for the shear speed in Eq. (A6), can be evaluated as a function of grain size with the aid of Eq. (A7). A family of curves will be obtained, each associated with a particular value of D. For a specific sediment, D may be estimated from Eq. (A7) if N and u_g are both available from experimental measurements.

Although the Hertz theory yields grain-size and sediment-depth dependencies that appear to align reasonably well with the few existing data sets, it may be found, as new data become available, that a better description of grain contact mechanics is required. For instance, the assumption that the grains are frictionless, which is central to the Hertz theory, may have to be relaxed. This, and other possible refinements to the treatment of the contact mechanics, could lead to grain-size and sediment-depth dependencies that differ from those in Eqs. (A2) and (A3). Corresponding differences would then be expected in the predicted wave speeds and attenuations as functions of grain size and sediment depth.

[1] M. A. Biot, ''Theory of propagation of elastic waves in a fluid-saturated porous solid: I. Low-frequency range,'' J. Acoust. Soc. Am. **28**, 168–178 (1956).

[2] M. A. Biot, ''Theory of propagation of elastic waves in a fluid-saturated porous solid: II. Higher frequency range,'' J. Acoust. Soc. Am. **28**, 179–191 (1956).

[3] R. D. Stoll, *Sediment Acoustics* (Springer-Verlag, Berlin, 1989), Vol. 26.

[4] C.-H. Liu and S. R. Nagel, ''Sound in sand,'' Phys. Rev. Lett. **68**, 2301–2304 (1992).

[5] C.-H. Liu, S. R. Nagel, D. A. Schecter, S. N. Coppersmith, S. Majumdar, O. Narayan, and T. A. Witten, ''Force fluctuations in bead packs,'' Science **29**, 513–515 (1995).

[6] M. J. Buckingham, ''Theory of acoustic attenuation, dispersion, and pulse propagation in unconsolidated granular materials including marine sediments,'' J. Acoust. Soc. Am. **102**, 2579–2596 (1997).

[7] M. J. Buckingham, ''Theory of compressional and shear waves in fluid-like marine sediments,'' J. Acoust. Soc. Am. **103**, 288–299 (1998).

[8] S. Granick, ''Soft matter in a tight spot,'' Phys. Today **52**, 26–31 (1999).

[9] J. Gittus, *Creep, Viscoelasticity and Creep Fracture in Solids* (Wiley, New York, 1975).

[10] H. M. Jaeger, S. R. Nagel, and R. P. Behringer, ''The physics of granular materials,'' Phys. Today **49**, 32–38 (1996).

[11] C.-h. Liu and S. R. Nagel, ''Sound in a granular material: disorder and nonlinearity,'' Phys. Rev. B **48**, 15646–15650 (1993).

[12] C.-h. Liu and S. R. Nagel, ''Sound and vibrations in granular materials,'' J. Phys.: Condens. Matter **6**, A433–A436 (1994).

[13] C.-h. Liu, ''Spatial patterns of sound propagation in sand,'' Phys. Rev. B **50**, 782–794 (1994).

[14] D. M. Mueth, H. M. Jaeger, and S. R. Nagel, ''Force distribution in a granular medium,'' Phys. Rev. E **57**, 3164–3169 (1998).

[15] S. R. Nagel and H. M. Jaeger, ''Sound propagation in sand,'' in *Echoes*, edited by T. Rossing (Acoustical Society of America, New York, 1998), Vol. 8, pp. 1, 4.

[16] A. Barbagelata, M. Richardson, B. Miaschi, E. Muzi, P. Guerrini, L. Troiano, and T. Akal, ''ISSAMS: An in situ sediment acoustic measurement system,'' in *Shear Waves in Marine Sediments*, edited by J. M. Hovem, M. D. Richardson, and R. D. Stoll (Kluwer, Dordrecht, 1991), pp. 305–312.

[17] S. R. Griffin, F. B. Grosz, and M. D. Richardson, ''*In situ* sediment geoacoustic measurement system,'' Sea Technol. , 19–22 (1996).

[18] M. D. Richardson, ''In-situ, shallow-water sediment geoacoustic properties,'' in *Shallow-Water Acoustics*, edited by R. Zhang and J. Zhou (China Ocean, Beijing, 1997), pp. 163–170.

[19] M. D. Richardson, personal communication, 1998.

[20] E. L. Hamilton, ''Compressional-wave attenuation in marine sediments,'' Geophysics **37**, 620–646 (1972).

[21] E. L. Hamilton, ''Acoustic properties of sediments,'' in *Acoustics and the Ocean Bottom*, edited by A. Lara-Saenz, C. R. Cuierra, and C. Carbo-Fité (Consejo Superior de Investigacions Cientificas, Madrid, 1987), pp. 3–58.

[22] A. B. Wood and D. E. Weston, ''The propagation of sound in mud,'' Acustica **14**, 156–162 (1964).

[23] L. Bjørnø, ''Features of the linear and non-linear acoustics of water-saturated marine sediments,'' Technical University of Denmark, Report No. AFM76-06, June 1976.

[24] M. C. Ferla, G. Dreini, F. B. Jensen, and W. A. Kuperman, ''Broadband model/data comparisons for acoustic propagation in coastal waters,'' in *Bottom-Interacting Ocean Acoustics*, edited by W. A. Kuperman and F. B. Jensen (Plenum, New York, 1980), pp. 577–592.

[25] S. D. Rajan, G. V. Frisk, and J. F. Lynch, ''On the determination of modal attenuation coefficients and compressional wave attenuation profiles in a range-dependent environment in Nantucket Sound,'' IEEE J. Ocean Eng. **17**, 118–128 (1992).

[26] C. McCann and D. M. McCann, ''A theory of compressional wave attenuation in noncohesive sediments,'' Geophysics **50**, 1311–1317 (1985).

[27] F. A. Bowles, ''Observations on attenuation and shear-wave velocity in fine-grained, marine sediments,'' J. Acoust. Soc. Am. **101**, 3385–3397 (1997).

[28] B. A. Brunson and R. K. Johnson, ''Laboratory measurements of shear wave attenuation in saturated sand,'' J. Acoust. Soc. Am. **68**, 1371–1375 (1980).

[29] B. A. Brunson, ''Shear wave attenuation in unconsolidated laboratory sediments,'' in *Shear Waves in Marine Sediments*, edited by J. M. Hovem, M. D. Richardson, and R. D. Stoll (Kluwer, Dordrecht, 1991), pp. 141–147.

[30] A. C. Kibblewhite, ''Attenuation of sound in marine sediments: A review with emphasis on new low frequency data,'' J. Acoust. Soc. Am. **86**, 716–738 (1989).

[31] W. I. Futterman, ''Dispersive body waves,'' J. Geophys. Res. **67**, 5279–5291 (1962).

[32] C. W. Horton, Sr., ''Dispersion relationships in sediments and sea water,'' J. Acoust. Soc. Am. **55**, 547–549 (1974).

[33] C. W. Horton, Sr., ''Comment on 'Kramers-Kronig relationship between ultrasonic attenuation and phase velocity' [J. Acoust. Soc. Am. **69**, 696–701 (1981)],'' J. Acoust. Soc. Am. **70**, 1182 (1981).

[34] M. O'Donnell, E. T. Jaynes, and J. G. Miller, ''General relationships

between ultrasonic attenuation and dispersion,'' J. Acoust. Soc. Am. **63**, 1935–1937 (1978).
[35] M. O'Donnell, E. T. Jaynes, and J. G. Miller, ''Kramers-Kronig relationship between ultrasonic attenuation and phase velocity,'' J. Acoust. Soc. Am. **69**, 696–701 (1981).
[36] E. Kjartansson, ''Constant *Q*-wave propagation and attenuation,'' J. Geophys. Res. **84**, 4737–4748 (1979).
[37] E. G. McLeroy and A. DeLoach, ''Sound speed and attenuation, from 15 to 1500 kHz, measured in natural sea-floor sediments,'' J. Acoust. Soc. Am. **44**, 1148–1150 (1968).
[38] C. McCann and D. M. McCann, ''The attenuation of compressional waves in marine sediments,'' Geophysics **34**, 882–892 (1969).
[39] D. J. Wingham, ''The dispersion of sound in sediment,'' J. Acoust. Soc. Am. **78**, 1757–1760 (1985).
[40] M. R. Wyllie, A. R. Gregory, and L. W. Gardner, ''Elastic wave velocities in heterogeneous and porous media,'' Geophysics **21**, 41–70 (1956).
[41] H. J. Simpson and B. H. Houston, ''A synthetic array measurement of a fast compressional and a slower wave in an unconsolidated water-saturated porous medium,'' J. Acoust. Soc. Am. **102**, 3210 (1997).
[42] H. J. Simpson and B. H. Houston, ''Analysis of laboratory measurements of sound propagating into an unconsolidated water-saturated porous media,'' J. Acoust. Soc. Am. **103**, 3095–3096 (1998).
[43] H. J. Simpson, B. H. Houston, and L. S. Couchman, ''Measurements and modeling of sound propagating into unconsolidated water-saturated porous media in a laboratory environment,'' J. Acoust. Soc. Am. **104**, 1787 (1998).
[44] H. J. Simpson and B. H. Houston, ''Synthetic array measurements of acoustical waves propagating into a water-saturated sandy bottom for a smoothed and a roughened interface,'' J. Acoust. Soc. Am. **107**, 2329–2337 (2000).
[45] T. J. Plona, ''Observation of a second bulk compressional wave in a porous medium at ultrasonic frequencies,'' Appl. Phys. Lett. **36**, 259–261 (1980).
[46] D. L. Johnson and T. J. Plona, ''Acoustic slow waves and the consolidation transition,'' J. Acoust. Soc. Am. **72**, 556–565 (1982).
[47] F. Gassmann, ''Über die elastizität poröser medien,'' Vierteljahrsscher. Naturforsch. Ges. Zürich **96**, 1–23 (1951).
[48] B. Bhushan, J. N. Israelachvili, and U. Landman, ''Nanotribology: friction, wear and lubrication at the atomic scale,'' Nature (London) **374**, 607–616 (1995).
[49] M. T. Bengisu and A. Akay, ''Stick-slip oscillations: Dynamics of friction and surface roughness,'' J. Acoust. Soc. Am. **105**, 194–205 (1999).
[50] M. J. Buckingham, *Noise in Electronic Devices and Systems* (Ellis Horwood, Chichester, 1983).
[51] S. O. Rice, ''Mathematical analysis of random noise,'' Bell Syst. Tech. J. **23**, 282–332 (1945).
[52] R. D. Mindlin, ''Compliance of elastic bodies in contact,'' J. Appl. Mech. **16**, 259–268 (1949).
[53] R. D. Mindlin, W. P. Mason, W. P. Osmer, and H. Deresiewicz, ''Effects of an oscillating tangential force on the contact surfaces of elastic spheres,'' presented at First National Congress on Applied Mechanics, Chicago, 1951.
[54] R. D. Mindlin and H. Deresiewicz, ''Elastic spheres in contact under varying oblique forces,'' J. Appl. Mech. **20**, 327–344 (1953).
[55] R. D. Mindlin, ''Mechanics of granular media,'' presented at Second U.S. National Congress on Applied Mechanics, Ann Arbor, 1954.
[56] P. G. Nutting, ''The deformation of granular solids,'' J. Wash. Acad. Sci. **18**, 123–126 (1928).
[57] H. Deresiewicz, ''Mechanics of granular matter,'' in *Advances in Applied Mechanics*, edited by H. L. Dryden and T. v. Kármán (Academic, New York, 1958), Vol. 5, pp. 233–306.
[58] A. L. Demirel and S. Granick, ''Glasslike transition of a confined simple fluid,'' Phys. Rev. Lett. **77**, 2261–2264 (1996).
[59] P. M. Morse and K. U. Ingard, *Theoretical Acoustics* (McGraw-Hill, New York, 1968).
[60] A. B. Wood, *A Textbook of Sound*, 3rd ed. (G. Bell, London, 1964).
[61] M. D. Richardson and K. B. Briggs, ''In situ and laboratory geoacoustic measurements in soft mud and hard-packed sand sediments: Implications for high-frequency acoustic propagation and scattering,'' Geo-Mar. Lett. **16**, 196–203 (1996).
[62] M. D. Richardson, ''Spatial variability of surficial shallow water sediment geoacoustic properties,'' in *Ocean-Seismo Acoustics: Low-Frequency Underwater Acoustics*, edited by T. Akal and J. M. Berkson (Plenum, New York, 1986), pp. 527–536.
[63] P. M. Morse and H. Feshbach, *Methods of Theoretical Physics: Part 1* (McGraw-Hill, New York, 1953), Vol. 1.
[64] M. D. Richardson, K. B. Briggs, D. L. Bibee *et al.*, ''Overview of SAX99: environmental considerations,'' IEEE J. Ocean. Eng. (in press).
[65] D. W. Bell and D. J. Shirley, ''Temperature variation of the acoustical properties of laboratory sediments,'' J. Acoust. Soc. Am. **68**, 227–231 (1980).
[66] J. M. Hovem and G. D. Ingram, ''Viscous attenuation of sound in saturated sand,'' J. Acoust. Soc. Am. **66**, 1807–1812 (1979).
[67] M. J. Buckingham, ''Precision correlations between the geoacoustic parameters of an unconsolidated, sandy marine sediment,'' J. Comput. Acoust. (in press).
[68] E. L. Hamilton, ''Elastic properties of marine sediments,'' J. Geophys. Res. **76**, 579–604 (1971).
[69] J. E. White and R. L. Sengbush, ''Velocity measurements in near-surface formations,'' Geophysics **18**, 54–69 (1953).
[70] S. P. Timoshenko and J. N. Goodier, *Theory of Elasticity*, 3rd ed. (McGraw-Hill, New York, 1970).
[71] M. D. Richardson, E. Muzi, B. Miashi, and F. Turgutcan, ''Shear wave velocity gradients in near-surface marine sediment,'' in *Shear Waves in Marine Sediments*, edited by J. M. Hovem, M. D. Richardson, and R. D. Stoll (Kluwer, Dordrecht, 1991), pp. 295–304.
[72] E. L. Hamilton, ''Shear-wave velocity versus depth in marine sediments: A review,'' Geophysics **41**, 985–996 (1976).
[73] O. K. Rice, ''On the statistical mechanics of liquids, and the gas of hard elastic spheres,'' J. Chem. Phys. **12**, 1–18 (1944).